

BIOMECHANICS OF LOWER LIMB DURING THE GOLF SWING USING OPENSIM
MODELING

A Thesis

by

ANDREW B. BUTLER

Submitted to the Graduate College of
The University of Texas Rio Grande Valley
In partial fulfillment of the requirements for the degree of

MASTER OF SCIENCE IN ENGINEERING

May 2019

Major Subject: Mechanical Engineering

BIOMECHANICS OF LOWER LIMB DURING THE GOLF SWING USING OPENSIM
MODELING

A Thesis
by
ANDREW B. BUTLER

COMMITTEE MEMBERS

Dr. Dumitru Caruntu
Chair of Committee

Dr. Robert Freeman
Committee Member

Dr. Javier Ortega
Committee Member

Dr. Dorina Chipara
Committee Member

May 2019

Copyright 2019 Andrew B. Butler

All Rights Reserved

ABSTRACT

Butler, Andrew B., The Biomechanics of the Lower-Limb During the Golf Swing Using OpenSim Modeling. Master of Science in Engineering (MSE), May, 2019, 68 pp., 43 figures, references, 54 titles.

The purpose of this research is to investigate the biomechanics of the lower-limb using an inverse dynamics model. Experimental data, recorded by an integrated Motion Analysis – Force Plate System in the UTRGV Biomechanics Laboratory, is used to determine ground reaction forces and marker trajectories. OpenSim, a graphical musculoskeletal and computational platform, is used to model the body in three dimensions. The human body is modeled as a 12-segment linkage, consisting of 23 degrees-of-freedom and 92 muscles. The experimental data for the Biomechanics Laboratory is imported in OpenSim. Then, joint angles, generalized coordinates & accelerations of lower-limb segments, muscle forces, joint torques, and reaction loads are determined using an inverse dynamics based approach. The motion under investigation is the golf swing. The model also investigates gait. Comparisons of the results with data reported in the literature are presented. Discussions on the novelty, applications, and limitations are also reported.

DEDICATION

The completion of my studies and this work would not have been possible without the love and support of my family. My mother, Kathryn Butler, my father, Alley C. Butler, my brothers, James and Thomas Butler, and sister-in law, Brittney Butler, inspired, motivated, and supported me by all means to accomplish this degree. Thank you for your love and patience.

ACKNOWLEDGEMENTS

I will always be grateful to Dr. Dumitru Caruntu, the chair of my thesis committee, for all his mentoring and advice. He has encouraged me to complete this process through his infinite patience and guidance. Many thanks go as well to my thesis committee members, Dr. Robert Freeman, Dr. Javier Ortega, & Dr. Dorina Chipara. Their advice, input and comments on my thesis helped to ensure the quality of my intellectual work. I would also like to thank Dr. Constantine Tarawneh, Dr. Robert Jones, and Dr. Horacio Vasquez for acting as mentors throughout my graduate studies.

I would also like to thank my colleagues at the UTRGV library who helped me locate supporting documents for my research. Also, I would like to acknowledge my peers in Dr. Caruntu's research laboratory that have helped me complete this thesis.

TABLE OF CONTENTS

	Page
ABSTRACT.....	iii
DEDICATION.....	iv
ACKNOWLEDGEMENTS.....	v
TABLE OF CONTENTS.....	vi
LIST OF TABLES.....	ix
LIST OF FIGURES.....	x
CHAPTER I. INTRODUCTION.....	1
1.1 Inverse Dynamics.....	2
1.2 Technologies & Applications.....	3
1.3 Purpose.....	3
CHAPTER II. REVIEW OF LITERATURE.....	5
2.1 Studies on Gait.....	5
2.1.1 Methods.....	6
2.1.2 Dynamic Events during Gait.....	6
2.1.3 Anthropometry.....	8
2.1.4 Recent Research.....	9
2.2 Studies on Golf.....	10
2.2.1 The Golf Swing.....	10
2.2.2 Recent Research.....	11

CHAPTER III. OPENSIM.....	15
3.1 General Inverse Dynamics Theory.....	16
3.2 Scaling in OpenSim.....	19
3.2.1 Computed Scale Factors.....	19
3.2.2 Geometric, Inertial, & Anatomical Scaling.....	20
3.3 Kinematics & Weighted-Least Squares.....	21
3.4 Inverse Dynamics and Static Optimization.....	22
CHAPTER IV. EXPERIMENTAL METHODS.....	25
4.1 Motion Capture.....	25
4.2 Setup.....	28
4.3 Processing Motion Capture Data.....	28
CHAPTER V. RESULTS.....	30
5.1 Biomechanics of Gait.....	30
5.1.1 Ground Reaction Forces.....	30
5.1.2 Joint Angles.....	32
5.1.3 Moments.....	33
5.1.3.1 Hip.....	34
5.1.3.2 Knee.....	35
5.1.3.3 Ankle.....	36
5.1.4 Muscle Force Estimations.....	37
5.1.5 Joint Reaction Forces.....	39
5.2 Biomechanics of Golf.....	41
5.2.1 Trailing vs. Leading Leg GRFs.....	41

5.2.2 Trailing vs. Leading Leg Joint Angles.....	44
5.2.3 Moments.....	45
5.2.3.1 Hip.....	45
5.2.3.2 Knee.....	49
5.2.4 Muscle Force Estimations.....	50
5.2.5 Joint Reaction Forces.....	52
CHAPTER VI. DISCUSSION	56
6.1 Conclusions from Motion Studies.....	56
6.2 Limitations of Current Work.....	58
6.3 Clinical Recommendations.....	59
REFERENCES.....	60
APPENDIX.....	64
BIOGRAPHICAL SKETCH.....	68

LIST OF TABLES

	Page
Table 1: Anthropometric Data (Winter, 2009).....	9

LIST OF FIGURES

	Page
Figure 1: A multiple camera, motion capture environment (Vicon Motion Systems, 2019).....	2
Figure 2: Phases of gait.....	7
Figure 3: Body segment lengths expressed in terms of height, H	8
Figure 4: Knee model with various ligaments present.....	9
Figure 5: Dynamic events during the golf swing.....	11
Figure 6: An instrumented prosthetic used to measure forces <i>in vivo</i>	13
Figure 7: An OpenSim musculoskeletal model.....	16
Figure 8: OpenSim scaling procedure.....	20
Figure 9: The UTRGV Biomechanics Laboratory.....	26
Figure 10: A VICON MX-T Series Camera.....	26
Figure 11: Reflective marker set.....	27
Figure 12: Two AMTI Force Plates used during motion capture.....	27
Figure 13: The MOtoNMS interface.....	29
Figure 14: GRF data for the leg during the walking exercise beginning with heel strike.....	31
Figure 15: Joint angles for the leg during the walking exercise beginning with heel strike.....	33
Figure 16: Joint moments in the hip during walking.....	34
Figure 17: Joint moments in the knee during walking.....	35
Figure 18: Joint moments in the ankle during walking.....	36

Figure 19: Force estimation in the thigh during stance.....	37
Figure 20: Force estimation in the shank during stance.....	38
Figure 21: Force estimations compared with Pandy & Andriacchi (2010).....	39
Figure 22: Peak loading at the hip joint during gait.....	40
Figure 23: Peak loading at the knee joint during gait.....	40
Figure 24: Peak loading at the ankle joint during gait.....	41
Figure 25: Ground reaction force data in the vertical direction during the golf swing.....	42
Figure 26: Ground reaction force data in the trailing leg during the golf swing.....	43
Figure 27: Ground reaction force data in the leading leg during the golf swing.....	44
Figure 28: Leading and trailing knee flexion angles during the golf swing.....	45
Figure 29: Joint torque data in the trailing leg hip during the golf swing.....	46
Figure 30: Joint torque data in the leading leg hip during the golf swing.....	47
Figure 31: Hip extensor moments for the trailing leg with comparison.....	47
Figure 32: Hip adduction moments for the trailing leg with comparison.....	48
Figure 33: Hip internal rotation moments for the trailing leg with comparison.....	48
Figure 34: Hip extensor moments for the leading leg with comparison.....	48
Figure 35: Hip adduction moments for the leading leg with comparison.....	49
Figure 36: Hip internal rotation moments for the leading leg with comparison.....	49
Figure 37: Joint torque in the knees during the golf swing.....	50
Figure 38: Force estimation in the trailing leg during the golf swing.....	51
Figure 39: Force estimation in the leading leg during the golf swing.....	52
Figure 40: Loading at the hip joint during the golf swing.....	53
Figure 41: Loading at the knee joint during the golf swing.....	54

Figure 42: Peak loading in the trailing knee during the golf swing.....54

Figure 43: Peak loading in the leading knee during the golf swing.....55

CHAPTER I

INTRODUCTION

The origins of modern biomechanics, and more specifically inverse dynamics, dates back to a 17th century Englishman. A former professor at the University of Cambridge, Isaac Newton devoted his life's work to developing ways of explaining how the world works. During his career, he generated mathematical formulations on universal gravitation, cooling and heat transfer, rheology, & optics, all of which have had a profound impact in their own fields as society has developed since that time. But perhaps his most notable contribution came from a publication in the late 1600s.

Newton's Principia in 1687 laid the groundwork for classical mechanics. In his publication, one of his axioms, which we now know as laws, effectively facilitates how engineers, physicians, and physical therapists understand biomechanics related phenomena. Newton's second law establishes that the forces acting on an object are proportional to the object's acceleration as a consequence of the object's inertia (Newton, 1687). Written differently, we have:

$$\sum \vec{F} = m\vec{a} \quad (1)$$

In Biomechanics, this equation is central to any inverse dynamics based approach. And for the work presented herein, it is the foundation from which the work originates.

1.1 Inverse Dynamics

Inverse dynamics is a branch of biomechanics that estimates muscle forces and moments from known kinematic and kinetic information. After collecting trajectories relative to various anatomical features using a motion capture system (**Fig. 1**), dynamic equations can be solved by calculating the appropriate accelerations. These are then used in conjunction with known external forces and weights in order to solve a system of equations.

Typically, there are more unknown variables in the system of equations than known variables. As such, the indeterminate system can be resolved by performing optimization. This is done by minimizing an objective function. In doing so, a suitable approximation can be achieved for a given model.

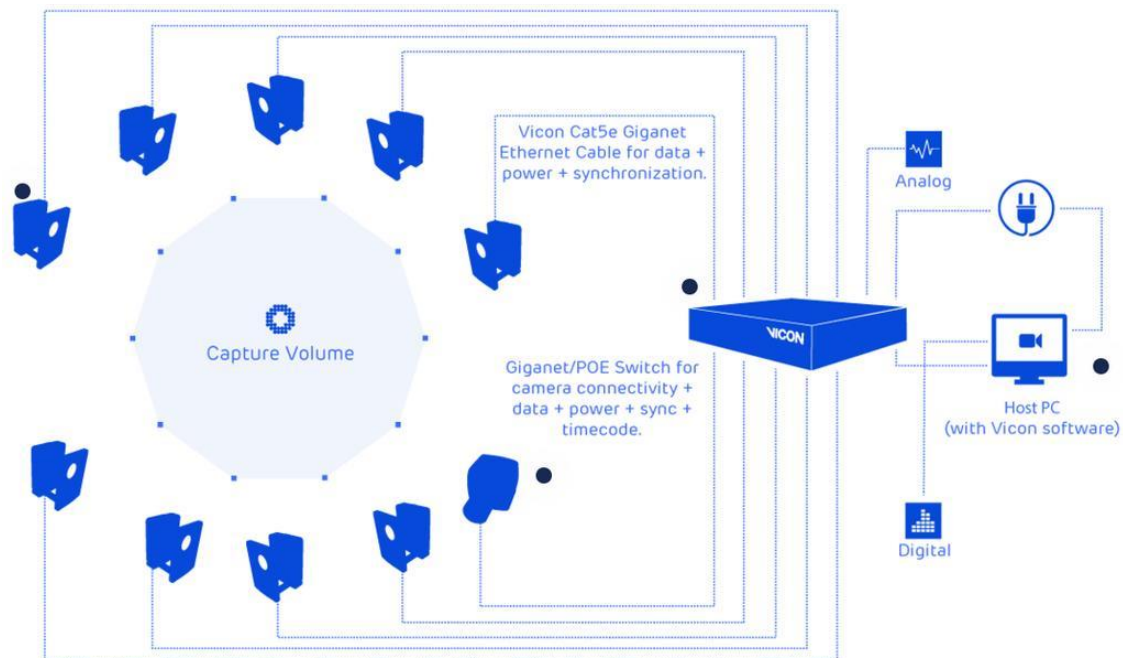


Figure 1: A multiple camera, motion capture environment (Vicon Motion Systems, 2019)

1.2 Technologies & Applications

Fortunately, advances in computing technologies have enabled researchers to leverage inverse dynamics and computer optimization with greater accuracy. Various musculoskeletal simulation and analysis packages, such as Anybody (Anybody Technology), Visual 3-D (C-Motion, Inc.), and SIMM (Motion Analysis, Corp.), enable a sophisticated investigation into human locomotion (Damsgaard et al., 2006; Erdemir, 2016; Delp et al., 1990). This is significant for clinicians or healthcare professionals that require greater analysis for clinical decision-making.

There are various applications of this work that can yield high impact in the community. Surgical planning, orthopedics, rehabilitation program development, scientific testing, and ergonomic product design are just a few benefits offered by using musculoskeletal analysis tools (Reinbolt et al., 2011; Seth et al., 2014; Escamilla et al., 2012; Rasmussen et al., 2003). The fundamental scientific process, i.e. hypothesis testing, can easily be simulated and observed. This is indeed a necessity as research costs and time spent in the laboratory can quickly add up. As such, there is a need to study the basic movement patterns associated with human motion. Complex movement can only be categorized once a fundamental understanding persists regarding basic ambulatory exercises.

1.3 Purpose

The purpose of this research was to investigate the biomechanics of the lower-limb during the golf swing using inverse dynamics. While some exercise recommendations exist as rehabilitation guidelines following joint replacement surgery, there are limited data-driven

conclusions for the golf swing (Kuster, 2002; Swanson et al., 2009). Baker et al. (2017) provided a comprehensive review of risk factors associated with the golf swing in relation to the knee. The prevalence of knee injuries in golf was established to be between 3-18%, indicating that there is indeed a need to examine the golf swing as an appropriate exercise for rehabilitation.

Additionally, the product of gait analysis studies have a strong influence on the development of design criteria for medical device technologies (Andriacchi & Hurwitz, 1997). Therefore, the motivation for performing the current investigation was two-fold: (1) to produce evidence-based information that would enable clinicians to recommend or prohibit golf as a rehabilitation exercise and (2) to aid in the development of design criteria for total hip arthroplasty (THA) and total knee arthroplasty (TKA) with special considerations for the kinematics and kinetics that the golf swing presents.

CHAPTER II

REVIEW OF LITERATURE

Literature in the field of biomechanics was surveyed in two aspects. The survey primarily focused on inverse dynamics based approaches with regards to biomechanics related investigations, although forward dynamics methods were not excluded outright. A secondary criterion for investigations into either OpenSim and/or motion were established. Their significance was determined arbitrarily during and after the review was completed, whereby the number of citations held weight during the literature collection process. The studies collected are primarily organized by motion.

2.1 Studies on Gait

Investigations into human walking have been performed for several decades. Braüne & Fischer (1899) performed one of the earliest three-dimensional, mathematical analyses of human gait. In their seminal work, they carefully considered mass distribution as it relates to body segments. Then, in the mid-to-late 20th century, more studies began to provide meaningful insight into the mechanics of the lower extremities. Bresler & Frankel (1950) leveraged a force-plate transducer to examine ground reaction forces. By incorporating this data with an analysis of limb segments in three dimensions, they were able to report forces and moments at the joints in the lower leg. Then, in the 1970's, muscle force contributions were presented (Morrison, 1970;

Hardt, 1978). The methods by which they were able to resolve muscle force estimations differed. But the latter began an approach for greater accuracy using optimization.

2.1.1 Methods

Historically, linear programming approaches were developed in order satisfy optimization criterion (Seireg & Arvihar 1975, Crowninshield et al. 1978, Patriarco et al. 1981). However, as computing technologies advanced, non-linear based objective functions were used more frequently in the analysis of the lower-limb (Collins 1995, Glitsch & Baumann 1997, Peterson 1997).

The rationale behind the minimization of a penalty function from a physiological standpoint, linear or non-linear, should be somewhat straightforward. Evolutionarily speaking, it is advantageous to expend the least amount of energy necessary to perform tasks, i.e. nothing more than what is necessary and sufficient should be expended (MacConaill 1966). Accordingly, modern day principles regarding how the objective functions are optimized in inverse dynamics are a reflection of that.

2.1.2 Dynamic Events during Gait

Because walking is a fundamental human movement, it is not surprising that a rich data set exists from experimentation. Accordingly, researchers explain gait in terms of various events related to movement patterns and when considering walking, it is useful to simplify these events within one cycle.

The starting point of an analysis is arbitrary, but a common approach identifies the beginning of the gait cycle when the heel of the foot strikes the ground first. This is known as heel-strike (HS). Then, as progression of the body weight moves forward, the following leg prepares to be airborne. The event just before this is known as contralateral toe-off (CTO). As this leg swings forward during the stance phase of gait, the complete body weight is supported solely on one leg. Once the leg being swung forward reaches and makes contact with the ground, contralateral heel strike (CHS) has occurred. The final event for the stance phase of gait occurs as the original leg prepares for liftoff from the ground. This event is known as toe-off (TO). These events summarize the stance phase of the gait cycle, as seen in **Fig. 2**. Once in the air, the leg enters the swing phase of the gait cycle, while the other leg repeats the gait cycle events for stance. This coordination of stance and swing make-up the human gait cycle. Stance is usually estimated to occur somewhere between 60-63% of the cycle, assuming heel strike is the first event.

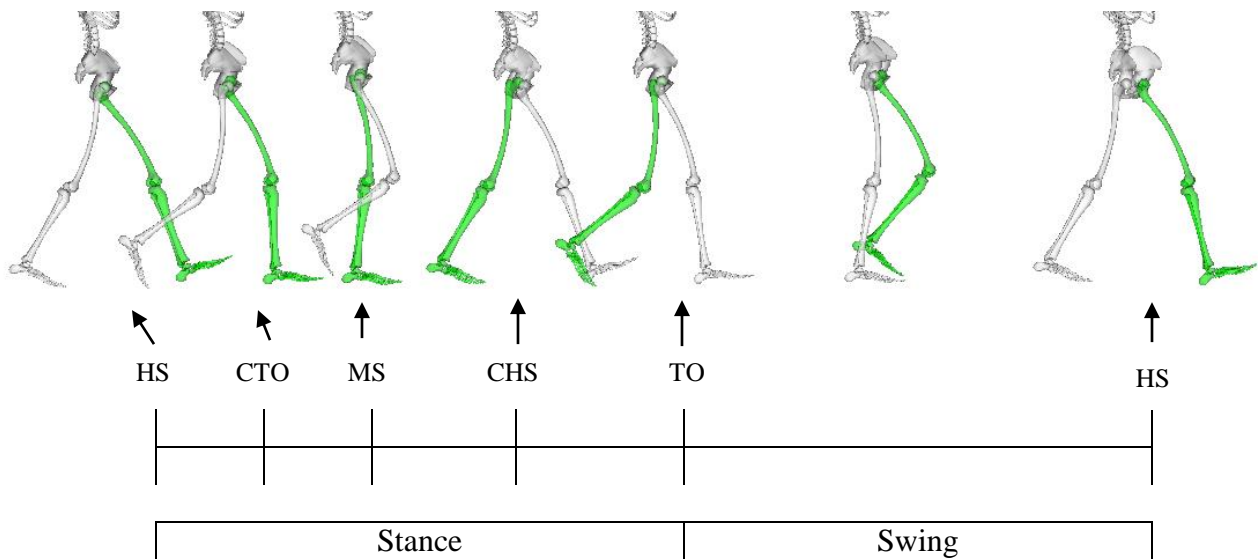


Figure 2: Phases of gait

2.1.3 Anthropometry

Anthropometry is a science that classifies body-segmental properties. This is critical in Biomechanics as the fundamental equations intrinsically require that segment masses or lengths are known, for example. Drillis and Contini (1966) have reported a codification system regarding segment lengths relative to body height (**Fig. 3**) which has facilitated the study of human body dynamics.

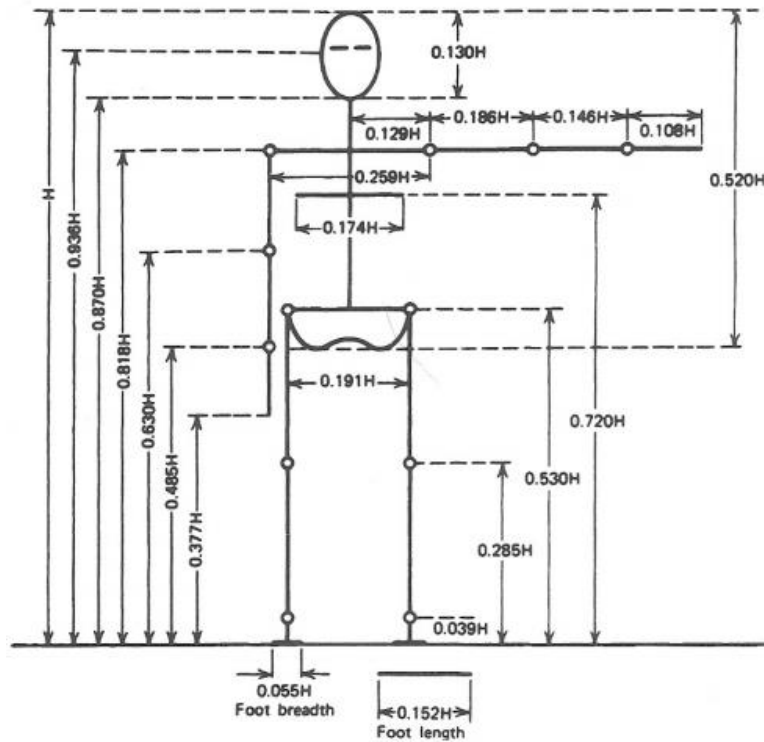


Figure 3: Body segment lengths expressed in terms of height, H (Drillis and Collins, 1966)

Similarly, masses and weights for segments of the body can be approximated from the total mass. For example, the thigh can be estimated to be approximately 40% of the total mass.

Table 1 indicates various properties associated common segments of the human body. While this

list is not extensive and not representative of the parameters used in this work, it does facilitate understanding that body-segmental masses are approximately proportional to body weight.

Table 1: Anthropometric Data (Winter, 2009)

Segment	Definition	Segment Weight/Total Body Weight	Center of Mass/Segment Length		Radius of Gyration		
			Proximal	Distal	C of G	Proximal	Distal
Foot	Lateral malleolus/head metatarsal II	0.0145	0.5	0.5	0.475	0.69	0.69
Leg	Femoral condyles/medial malleolus	0.0465	0.433	0.567	0.302	0.528	0.643
Thigh	Greater trochanter/femoral condyles	0.1	0.433	0.567	0.323	0.54	0.653
HAT	Greater trochanter/glenohumeral joint	0.678	0.0626	0.374	0.496	0.798	0.621

2.1.4 Recent Research

There are a few excellent reports in the field that currently exist. Erdemir and others (2007) provide numerous examples of investigations into various motions: walking, running, and upper body movements. Shelburne et al. (2004) also provide insight into the history of walking related studies, while their focus tended to investigate ACL loading during gait (**Fig. 4**). Other reviews that examine walking speed or effects of obesity on lower extremity dynamics exist (Liu et al., 2008; Browning & Kram, 2007).

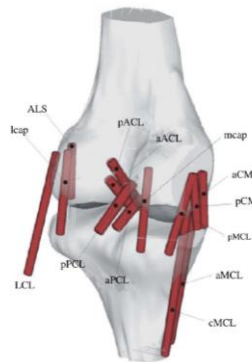


Figure 4: Knee model with various ligaments present (Shelburne et al., 2004)

And even though inverse dynamics based approaches can be useful in orthopedic applications, a recent focus in the community has been on dynamic optimization (Zajac et al., 2006). Muscle driven simulations can provide more accurate representations of muscle excitation patterns (Shelburne et al., 2004; Neptune et al., 2001; Pandy & Andriacchi, 2010; Shelburne et al., 2006; Shelburne et al., 2005). The drawback for forward dynamics driven simulations though is that they are expensive in computing time (Anderson & Pandy, 2001a). Nevertheless, either approach can typically provide satisfactory results. For example, a static and dynamic optimization solution of gait was compared and identified as all but equivalent (Anderson & Pandy, 2001b).

2.2 Studies on Golf

2.2.1 The Golf Swing

Similar to gait, the golf swing can be independently investigated. For the investigation presented herein, the motion of the golf swing was characterized by 3 phases and 4 specific events, as seen in **Fig. 5**. The golfer begins the motion in the starting pose. This is known as “address”. The golfer then brings the club through the backswing. The apex of the backswing describes the second distinct event. Then, the golf club is brought toward the ball in an explosive event, known as the downswing. As the golf club strikes the ball, known as “impact”, the momentum of the body rotates the stance towards the termination of the swing. This is colloquially known as follow-through. There is also naming convention for legs, to avoid confusion between handedness of golfers. The back leg of the golf swing is known as the trailing leg. The front leg of the golfer is sometimes known as the leading or target leg.

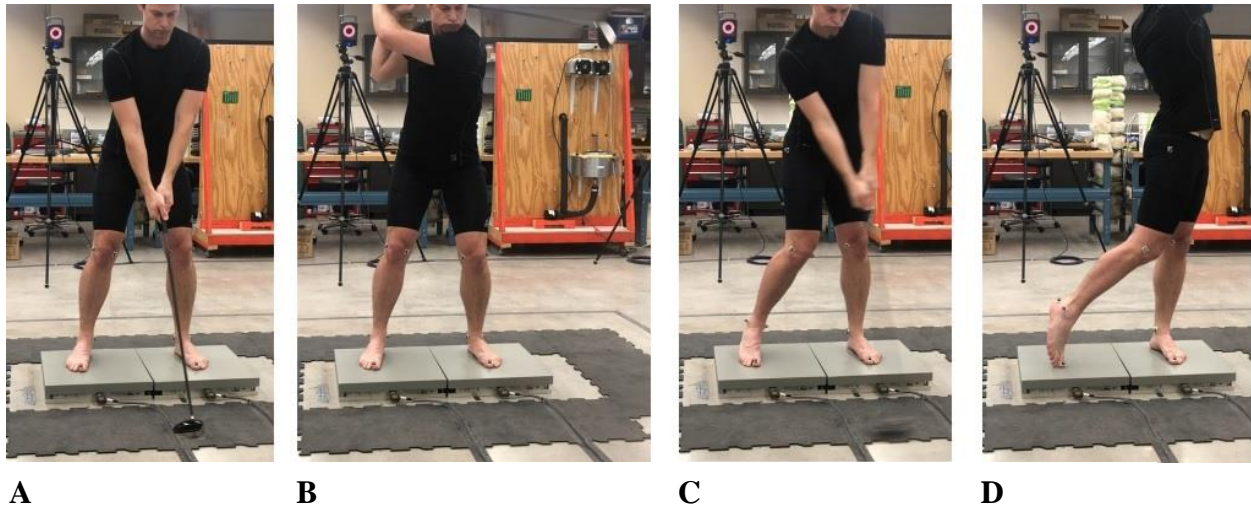


Figure 5: Dynamic events during the golf swing

2.2.2 Recent Research

Recent research from Foxworth et al. (2013) is very relevant to the present work. The purpose of their study was to compare the three-dimensional hip torques that exist during the golf swing between a younger male population and an older population of golfers. A set of 20 male golfers were separated into two groups, an older and younger population. The age of the older population was 56.9 ± 4.7 years and the age of the younger population was 25.1 ± 3.1 years. All subjects recorded 10 golf swings with their own driver using a motion capture system that collected kinematic and kinetic data. Inverse dynamics was executed and the 3-D hip joint torques were compared. They discovered that the hip joint moments in each plane were essentially indistinguishable by age, possibly because all golfers displayed a relative skill level or a maintained “strength” in the older population.

The kinetics of the knee joint were investigated by Gatt et al. (1998). The influence of shoe-type and skill level were considered in their work. Similar to Foxworth and the present work, a three-dimensional inverse dynamics based analysis was performed whereby a motion

capture system, including force plate data, was leveraged for computations. They concluded that the mean peak forces and moments that they calculated were significantly different between the lead and trail knees during the golf swing, but that loads were not significantly influenced by shoe type. And only the lead knee flexion and rotation moments were correlated to skill level. The basis of their work indicates that the characteristics of the golf swing are indeed fairly standard. It was also revealed that the magnitudes of the loading seen at the knee during the golf swing were similar to those that are prohibited until late-stage knee rehabilitation.

The medical community has the ability to receive benefits not only from mathematical models produced from inverse or forward dynamics based calculations, but also benefits from instrumented prosthetics. A study performed by D’Lima et al. (2008) investigated knee forces and moments *in vivo* using an instrumented prosthetic (**Fig. 6**). They implanted three patients with a tibial prosthetic that was instrumented with strain gauges and measured kinetic information for both exercise and recreational activities. In doing so, they were able to provide the clinical community with quantitative, evidence-based information regarding which activities should be recommended following total knee arthroplasty (TKA). An added benefit from their research was that design and failure analysis of prosthetics could be improved from the information they collected.



Figure 6: An instrumented prosthetic used to measure forces *in vivo* (D’Lima et al., 2008)

With respect to the golf swing motion, they reported peak tibial forces that were between 300-500% BW for the knees, with the leading knee carrying more load. They also reported the differences between using a sand wedge and a driver, with no significant difference observed. Their instrumented prosthetic effectively served as a ground force plate in the knee: compressive loads were examined from three orthogonal forces and three moments. As such, for analytical considerations, these could be seen as contact forces in the knee. Work from the same research group examined the golf swing and provided similar results for kinetics at the knees (Mündermann et al., 2008).

Other reports that have been produced investigate joint flexion angles or EMG activity but are limited in that they do not explicitly report muscular force in relation to loading at the

joints (Pfeiffer et al., 2014; Choi et al., 2014; McHardy & Pollard, 2005; Bechler et al., 1995).

There is no doubt that useful information from their work however exists in comparing with future work.

CHAPTER 3

OPENSIM

OpenSim is an open-source platform for generating and performing dynamic musculoskeletal simulations and analysis. This software was created with the intent of addressing pathological movement and exploring human body mechanics. One of the benefits that OpenSim offers is the extension to the user. Individuals can create their own analyses and plug-ins in C++ that are compatible with the current architecture (Delp et al., 2007).

Arguably, its greatest asset however is being able to incorporate motion capture data from the laboratory and perform a subsequent analysis. The software is an integrated engine that streamlines calculations through various modules (Delp & Loan, 2000). The graphical user interface is intuitive with functionality that can be extended through extensible markup language (XML). Integrating laboratory data into the software requires the appropriate conditioning and pre-processing with third-party applications, which can readily be done with the tools created from OpenSim contributors. Musculoskeletal simulations can be implemented both with muscle-driven controls, forward dynamics, and from kinematic and kinetic data, inverse dynamics. The structure and complexity of any given OpenSim model is dependent on the application, but typically these models will describe the human body as having multiple degrees-of-freedom and several musculotendon units (**Fig. 7**). For a thorough description of the base characteristics for OpenSim models, please see Appendix A.

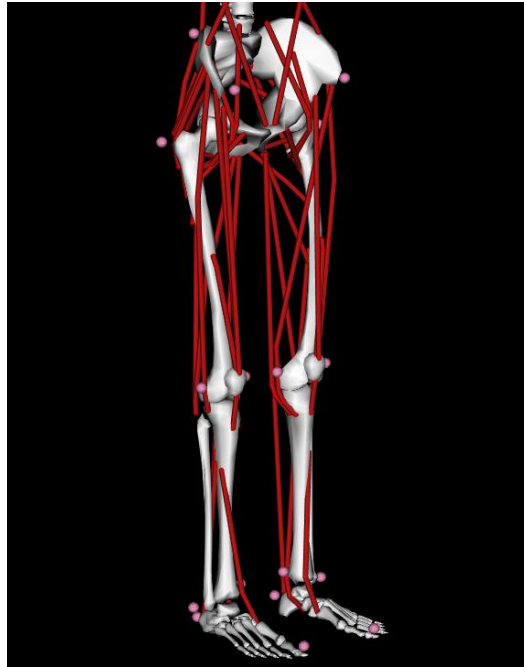


Figure 7: An OpenSim musculoskeletal model

With respect to anatomical considerations, the platform is robust. Bones can be modeled singularly as one body or as a collection. There is the capability to retain physical considerations such as mass, center of mass (COM), and moment of inertia about various axes. Muscles can also be modeled with a fair degree of precision relative to the human body. Insertion point, maximum isometric force, fiber length, and contraction velocity are just some parameters that can be modulated.

3.1 General Inverse Dynamics Theory

The process of estimating muscle forces, joint torques, or contact forces begins by collecting data from markers in three-dimensional space. The trajectory for each marker is captured in a given dimension and is recorded over time. Because we know that the first

derivative of position with respect to time is velocity (Eq. 2), we can use these markers to calculate the velocity of any segmental link center of mass (COM) at any point in time:

$$v = \frac{dx}{dt} \quad (2)$$

Similarly, for the second derivative (Eq. 3), the acceleration of any given link COM:

$$a = \frac{dv}{dt} = \frac{d^2x}{dt^2} \quad (3)$$

The combination of each acceleration vector can then fully describe any marker in the fixed global coordinate system.

Similarly, segmental (or link) angular accelerations are computed this way. An inverse kinematic approach is executed to collect joint angles by using a pre-determined coordinate system and the marker data collected therein. The markers themselves define the limbs which are then used in turn with trigonometry to calculate joint angles. The first and second derivative of these joint angles yields the angular velocity and angular acceleration, respectively.

Often however, the kinematic data from the markers themselves cannot be used without conditioning. There is inherent noise in the data that was collected from the markers. This is why typically in biomechanics, a 4th order, zero-phase lag Butterworth filter is used to smooth data and reduce the inaccuracies that are generated as a result of signal processing.

An object's translational and rotational inertia are also integral. With an object's mass known, and its acceleration derived, muscle force estimations and joint torque calculations can be made from the set of Newton-Euler equations:

$$\sum \vec{F}_{x_i} = m_i \vec{a}_{x_i} \quad (4)$$

$$\sum \vec{F}_{y_i} = m_i \vec{a}_{y_i} \quad (5)$$

$$\sum \vec{F}_{z_i} = m_i \vec{a}_{z_i} \quad (6)$$

$$\sum \vec{M}_{x_i} = I_i \vec{\alpha}_{x_i} \quad (7)$$

$$\sum \vec{M}_{y_i} = I_i \vec{\alpha}_{y_i} \quad (8)$$

$$\sum \vec{M}_{z_i} = I_i \vec{\alpha}_{z_i} \quad (9)$$

In Eqs. 5-10, inertial considerations for the i^{th} link, m_i and I_i , mass and moment of inertia, respectively, are known from anthropometry while each component of translational and rotational acceleration for the i^{th} link, a_i and α_i are calculated from motion capture trajectories.

Usually however this is not a very straightforward process. Depending on the methodology being used to estimate either forces or moments, typically there are more equations with unknown variables than there are known variables, or rather, an indeterminate system arises. No solution is inherently straightforward so typically an objective or cost function is minimized in order to obtain a solution that satisfies all the constraints necessary.

$$\min J = \sum_{m=1}^n F_m^p \quad (10)$$

In this optimization problem, the cost function J is minimized to a set of constraints. Typically, the sum of the forces, F , are raised to a power, p , where quadratic and cubic powers are common.

Kinetic information obtained during motion capture is used as input data to the inverse dynamics model (OpenSim Documentation, 2019). Specifically, force plates are used to collect ground reaction forces and moments, and centers of pressure. Similar to kinematic data, these too are subject to low-pass filtering for noise reduction.

3.2 Scaling in OpenSim

Another useful feature of the OpenSim software is the ability to model reflective markers. Using the three-dimensional virtual environment, pink data markers are represented in space relative to certain bodies. This is an important parameter in the modeling process as even slight variations can lead to strong deviations in muscle force estimations. In fact, typical tolerances between virtual and experimental markers are recommended to maintain an error in the range of 1-2 cm (OpenSim Documentation, 2019). The experimental markers are what enable an analysis to go to completion.

3.2.1 Computed Scale Factors

Scaling in OpenSim leverages both virtual and experimental markers in order to match a subject to a model. These measured distances, in addition to or in replacement of manually specified scale factors, will generate a musculoskeletal model specific to an individual person. During the computation of the scaling factors, the distance between x-y-z virtual markers in a default pose are compared to experimental data (**Fig. 8**). These values are averaged over a time period and are related such that the scale factor is proportional to the experimental marker pair distance and inversely proportional to the virtual marker pair distance (OpenSim Documentation, 2019):

$$S_1 = \frac{e_1}{m_1} \quad (11)$$

Here, s is the scale factor for a pair of markers, e is the experimental distance between marker pairs, and m is the virtual distance between marker pairs. The overall scale factor for a segment takes the averages of the scale factors for all marker pairs.

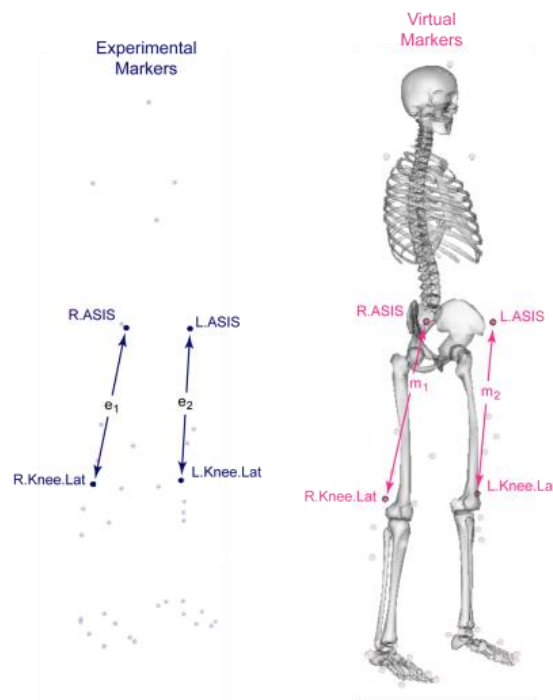


Figure 8: OpenSim scaling procedure (OpenSim Documentation, 2019)

3.2.2 Geometric, Inertial, & Anatomical Scaling

Several features are modified during the scaling procedure. First, a model's geometry, which includes COM, muscle insertion points, and joint frame locations, are scaled. These are scaled with respect to a specific segment, not the overall scale factor. Several options for the inertial scaling of segments and body mass exist. The most straightforward option for using

experimental data in OpenSim requires the mass distribution to be preserved. In doing so each body mass is scaled from scale factors, then once more by a ratio of the input mass and the sum of the scaled masses (OpenSim Documentation, 2019). For example, if in a general model the mass of the shank is half that of the femur, the scaled model for preserving mass distribution will also require this property, while maintaining that the overall mass equal the input mass (Winter, 2005). Lastly, features such as muscle length, or other relevant anatomical characteristics, are also scaled during the scaling procedure.

3.3 Kinematics & Weighted-Least Squares

Once a musculoskeletal model has been scaled, the virtual markers on a musculoskeletal model are then moved to best match the experimental markers. This is accomplished by stepping through a series of frames for a given motion. In doing so, generalized coordinate values are also generated.

The generation of experimental kinematics in OpenSim of movement from motion capture data follows a weighted least-squares approach (OpenSim Documentation, 2019):

$$\min_{\mathbf{q}} \left[\sum_{i \in \text{markers}} w_i \|\mathbf{x}_i^{\text{exp}} - \mathbf{x}_i(\mathbf{q})\|^2 + \sum_{j \in \text{unprescribed coords}} \omega_j (q_j^{\text{exp}} - q_j)^2 \right] \quad (12)$$

Here, marker positions corresponding to the vector of generalized coordinates \mathbf{q} is compared with the experimental position of marker i . The difference between the experimental position of a given marker, $\mathbf{x}_i^{\text{exp}}$, and it's position on the model is weighted by w_i . Similarly, the difference between experimental coordinate values, q_j^{exp} , and those computed from the built-in solver, q_j , makes an impact on the weighted least squares algorithm. The quadratic programming solver's default settings are a convergence criterion of 0.0001 and a limit of 1000 iterations. Because no

experimental coordinate values were used for this work, the entire second half of Eq. 22 disappears.

3.4 Inverse Dynamics and Static Optimization

Once the kinematics from motion capture are processed in OpenSim, the kinetics regarding a motion can then be explored. An OpenSim model will contain any number of degrees-of-freedom (dof), depending on how a model is constructed. Some of the common models in OpenSim are composed of either 10 dof or 23 dof. These degrees of freedom can completely describe the motion of the model at any point in time, primarily because the generalized coordinates are independent of one another.

In rigid-body mechanics, classical techniques regarding the analysis of multi-body systems typically will employ parameters that are convenient to use, such as generalized coordinates, and that have relation to a specified reference frame. In doing so, a system can be described analytically in the most simplest of terms. These derived equations of position using generalized coordinates facilitate velocity and acceleration derivations as well.

Accordingly, OpenSim uses the classical equations of motion to solve for kinetic parameters (OpenSim Documentation, 2019):

$$\mathbf{M}(\mathbf{q})\ddot{\mathbf{q}} + \mathbf{C}(\mathbf{q}, \dot{\mathbf{q}}) + \mathbf{G}(\mathbf{q}) + \mathbf{A}(\mathbf{q}, \dot{\mathbf{q}}, t, \mathbf{x}) = \boldsymbol{\tau} \quad (13)$$

In Eq. (13), $\mathbf{M}(\mathbf{q})$ represents the system mass matrix which is a function of the generalized coordinate vector, \mathbf{q} , representing position in three dimensional space. The acceleration term, $\ddot{\mathbf{q}}$, is a vector expression, in addition to the velocity vector, $\dot{\mathbf{q}}$. $\mathbf{C}(\mathbf{q}, \dot{\mathbf{q}})$ and $\mathbf{G}(\mathbf{q})$ represent the

contributions from Coriolis & centrifugal effects and gravitational forces, respectively.

$\mathbf{A}(\mathbf{q}, \dot{\mathbf{q}}, \mathbf{t}, \mathbf{x})$ is a vector of applied loads, or for this investigation, the ground reaction forces. All of the terms on the left-hand side of the expression are known a priori. The vector of generalized forces, i.e. torques, $\boldsymbol{\tau}$, is what inverse dynamics aims to compute. These are the moments about the generalized coordinates of the system, and in relevance to lower-limb biomechanics, the torques about the hip, knee, and ankle joints.

Estimating muscle forces becomes a bit more complex, from a mathematical standpoint. Because typically a musculoskeletal model will employ more muscles than degrees of freedom, the situation arises where an indeterminate system exists. Or rather, there are more unknowns than known variables in the equations. As such, there are an infinite number of potential solutions. In order to resolve systems such as these, the optimization (typically minimization) of an objective (cost) function is performed. This objective function typically includes each muscle's contribution.

In OpenSim, the objective function actually minimizes muscle force activations. This is accomplished primarily because the properties of the muscles do not change (OpenSim Documentation, 2019):

$$J = \sum_{m=1}^n (a_m)^p \quad (14)$$

Here, the activations, a , are minimized for the m through n^{th} muscle, which are summed together after raising each activation to a power, p . For the work presented herein, the selection of p was always 2. This function effectively represents each muscles contribution to motion vis-à-vis its activation. The constants of the muscle, i.e. insertion point, contraction velocity, maximum

isometric force, and physiological cross-sectional area (PCA), show up in the constraint equations (OpenSim Documentation, 2019):

$$\sum_{m=1}^n [a_m f(F_m^0, l_m, v_m)] r_{m,j} = \tau_j \quad (15)$$

Here, the constraint equation provides insight into how the system completely resolves muscle activation, a , from torques, τ , that are known from the classical equations of motion. The moment arm, $r_{m,j}$, is already prescribed in the model, in addition to the maximum isometric force, F_m^0 , length, l_m , and velocity, v_m , which come from a surface profile already characterized (Zajac, 1989). These characteristics enable the activations to be minimized in Eq. (14). In OpenSim, this is the “physiological case”. However, the ability to constrain the objective function based solely off of maximum isometric force, or what is referred to as ideal force generators, is possible. For the work presented herein, the former was always used.

CHAPTER IV

EXPERIMENTAL METHODS

4.1 Motion Capture

Typically, at least in experimental biomechanics, position information is collected from a series of reflective markers using a multiple camera arrangement. These cameras are usually oriented in a capture volume that will typically house any movements that are of interest. They use infrared radiation to bounce light off of the reflective markers and subsequently record their position in space. Their position in space is usually predetermined to a global reference frame. Usually researchers will establish a global coordinate system that is convenient for them and their work.

A motion capture analysis system was used to collect kinematic and kinetic information (**Fig. 9**). In the laboratory arrangement, 10 Vicon Nexus MX-T Series cameras (Vicon Motion Systems, Inc.) were used. These cameras operate by shining infrared light on reflective surfaces (**Fig. 10**). The coordinates of these reflective surfaces are then captured by the camera arrangement. These cameras were used to collect trajectories from 18 reflective markers. These markers were placed over bony landmarks and other identifiable anatomical features. The marker set was restricted to the lower-body, with several markers being placed over the waist, thighs, shanks, ankle, and feet (**Fig. 11**). The experimental marker positions were easily transferrable

into OpenSim, which enabled the subsequent analysis. The cameras sampled data at 100 Hz. Two AMTI (Advanced Mechanical Technology, Inc.) force plates were used that sampled data at 1000 Hz (**Fig. 12**).



Figure 9: The UTRGV Biomechanics Laboratory



Figure 10: A VICON MX-T Series Camera

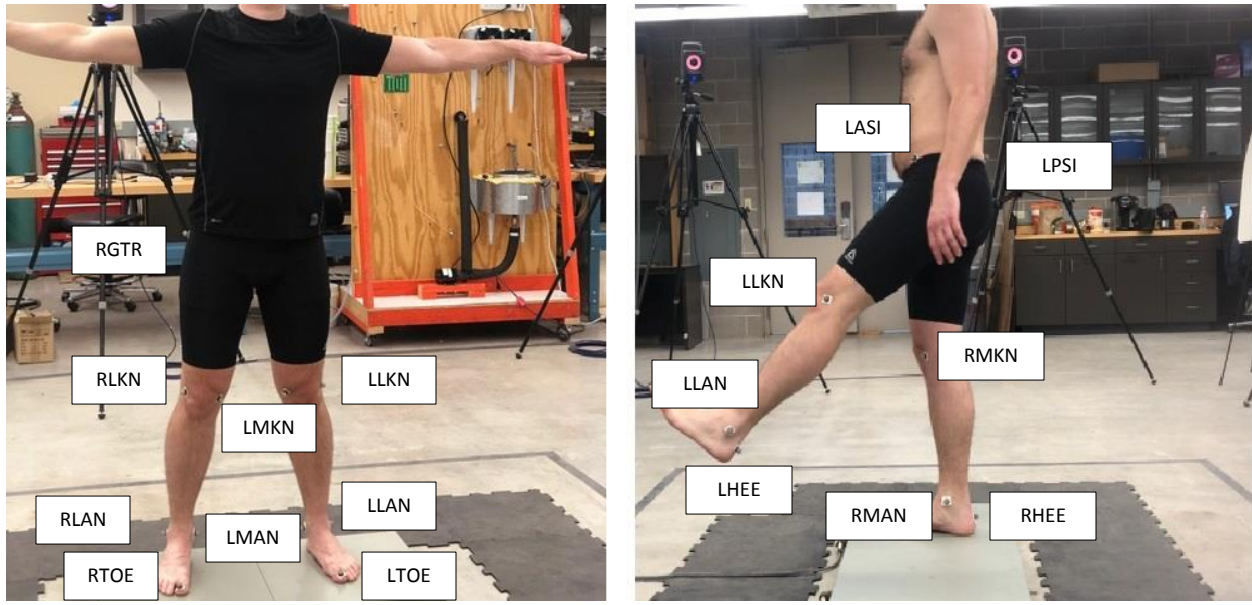


Figure 11: Reflective marker set

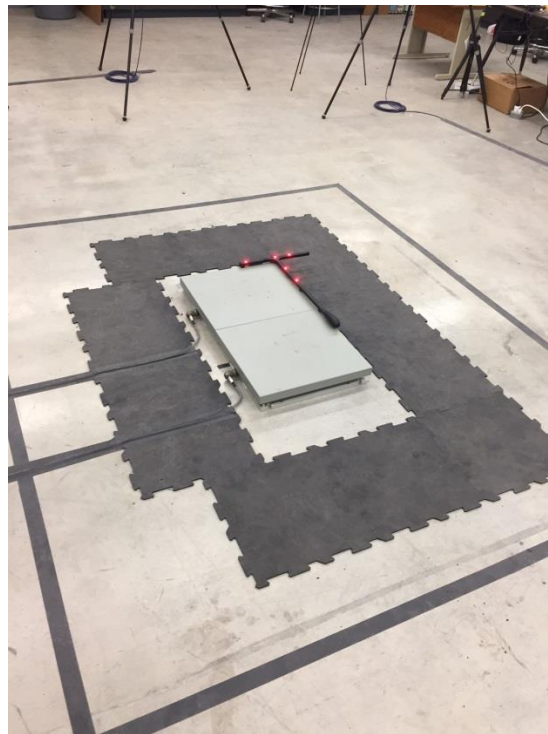


Figure 12: Two AMTI Force Plates used during motion capture

4.2 Setup

No shoes were worn during experimentation. Age and mass of the participant was 29 years & 100 kg. For walking trials, lumber (2"x4") was put together in front and behind the force plates so that the participant struck the force plates at the same height and left at the same height. The participant walked at a self-selected speed for comfortable walking. The force plates were physically adjusted to stride length, such that the participant would not need to compensate.

The skill level of the participant was a beginner golfer. The golf club used during motion capture was a 7-iron. The participant executed practice swings prior to execution. The participant visualized the golf ball, facilitating the golf swing motion.

4.3 Processing Motion Capture Data

Once information from the motion capture system was collected, a toolbox was used to process and convert data suitable for OpenSim (Mantoan et al., 2015). This toolbox is colloquially known as the Motion Data Elaboration Toolbox for Neuro-musculoskeletal Applications (MOtoNMS). The toolbox is maintained in MATLAB (Mathworks, Inc.) and fully enables an exploration of biomechanical information. Additionally, a biomechanical toolkit was used as a supplement to this toolbox (Barre & Armand, 2014). The general architecture can be seen in greater detail (**Fig. 13**).

Within the MOtoNMS toolbox, there are effectively three main sub-blocks that fully identify and extract meaningful information that OpenSim can use. The first module is known as the Acquisition Interface. This component of the MOtoNMS toolbox seeks to understand how

the biomechanical information was collected before it can be manipulated. Some of the various components that are of particular interest are the type and number of force plates used, the sampling frequencies, the marker set configurations, laboratory coordinate system configurations, plate padding, EMG setup, and more.

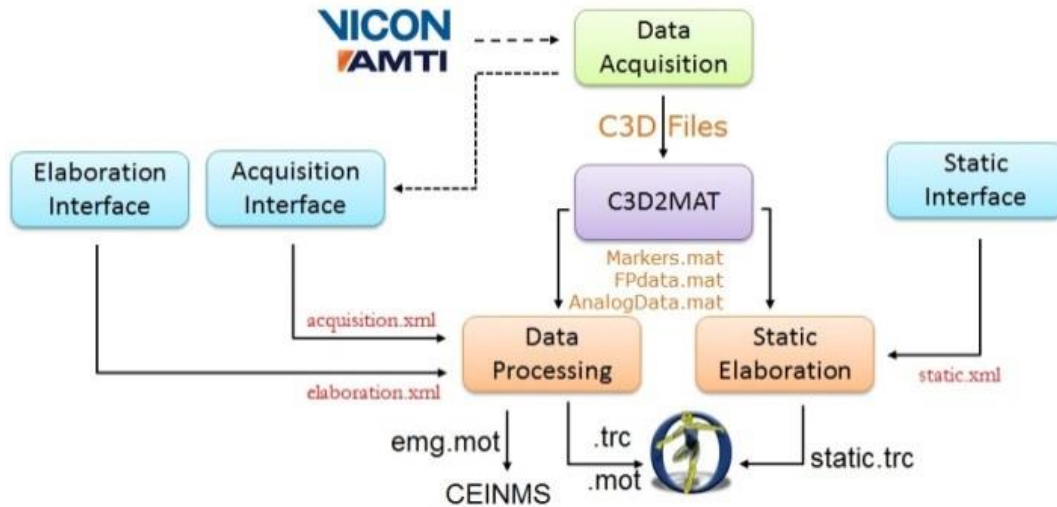


Figure 13: The MOtoNMS interface

The second and most straightforward interface is the C3D2MAT data structure. This block organizes all of the information that was collected from the Acquisition Interface into coherent MATLAB structures. The third and final sub-component of the MOtoNMS toolbox is the elaboration interface. This is arguably to most important component as the outputs are what are directly used in OpenSim calculations. Here, markers as well as the appropriate analyses are selected such that dynamic laboratory trials can be completely described. When relevant, EMG information is described here. For the purposes of the investigation at hand however, EMG recordings were not used.

CHAPTER V

RESULTS

The results presented in this section emanate from an analysis performed on the motions of walking and the golf swing. The focus of the results are on the lower extremities. Various dynamics related information is presented, such as ground reaction forces, joint angles, joint torques, muscle force estimations, and joint contact forces. For various phenomena, comparisons are made to previously published results in the literature. In particular to gait, only the stance phase was considered and analyzed.

5.1 Biomechanics of Gait

5.1.1 Ground Reaction Forces

The ground reaction force (GRF) during gait is presented in **Fig. 14**. The graph displays the ground reaction force contributions for each dimension. The figure itself is normalized with respect to body weight, which is a common practice in Biomechanics. It enables comparison and provides greater insight into the features of musculoskeletal dynamics. In **Fig. 14**, the dynamic events as described in **Fig. 2** are present at the top of the graph.

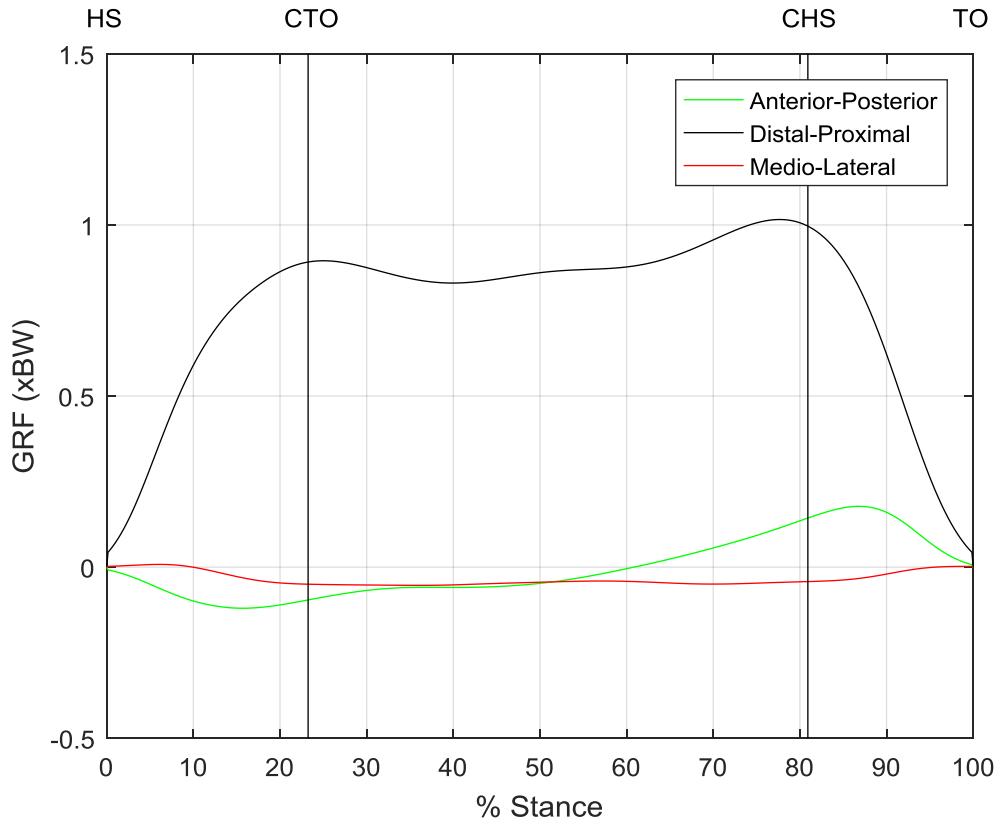


Figure 14: GRF data for the leg during the walking exercise beginning with heel strike

As the leg enters the stance phase of the gait cycle (**Fig.2**), weight is gradually shifted onto the leg, which leads to the large ground reaction force in the vertical direction, displayed by the proximal-distal curve. There are two large peaks for this curve that occur just after contralateral toe-off and right before contralateral heel strike. This is indicative of the leg in contact with the ground maintaining complete weight acceptance. The magnitudes of the curves themselves approach peaks of slightly greater than body weight, which is common. Additionally, during the stance phase, weight is shifted anteriorly. That is, a reaction force is exhibited posteriorly at the heel (initially) and gradually progresses to the front of the foot right before toe-off. The magnitude is small, relative to the vertical ground reaction force. Lastly, a reaction force

is initially present laterally, or directing outwards, at the beginning of the stance phase of the gait cycle, but quickly transitions inward in the medial direction, near contralateral toe-off.

5.1.2 Joint Angles

The calculated joint angles match well with other previously reported investigations (Collins, 1995; Liu et al., 2008). **Fig. 15** displays the joint angles during the stance phase of gait for the hip, knee, and ankle in the sagittal plane. At each joint, the direction of flexion/extension is worth noting. At the hip joint, during heel strike, the hip is flexed initially near 25° . As the leg progresses through stance, the leg reduces in flexion towards extension, decreasing in value, until contralateral heel strike, where a minimum is observed near this event. At toe-off, the flexion angle is already approaching that of heel strike as the leg is swung forward. The knee joint also maintains positive flexion for a majority of the stance phase of the gait cycle. A local maximum in flexion is observed near contralateral toe-off, with the largest flexion occurring during the swing phase. Ankle dorsiflexion, or the flexion of the ankle towards the ventral part of the body, is positive in **Fig. 15**. The kinematics of the ankle joint initially begin with plantar flexion as the leg establishes contact with the ground for the first 20-30% of gait. Then, after contralateral toe-off, the leg experiences a positive dorsiflexion as the leg nears toe-off. But right before, the foot must propel the body forward and so a large, rapid decrease in the ankle flexion (plantar flexion) angle is observed with a peak occurring during the swing phase.

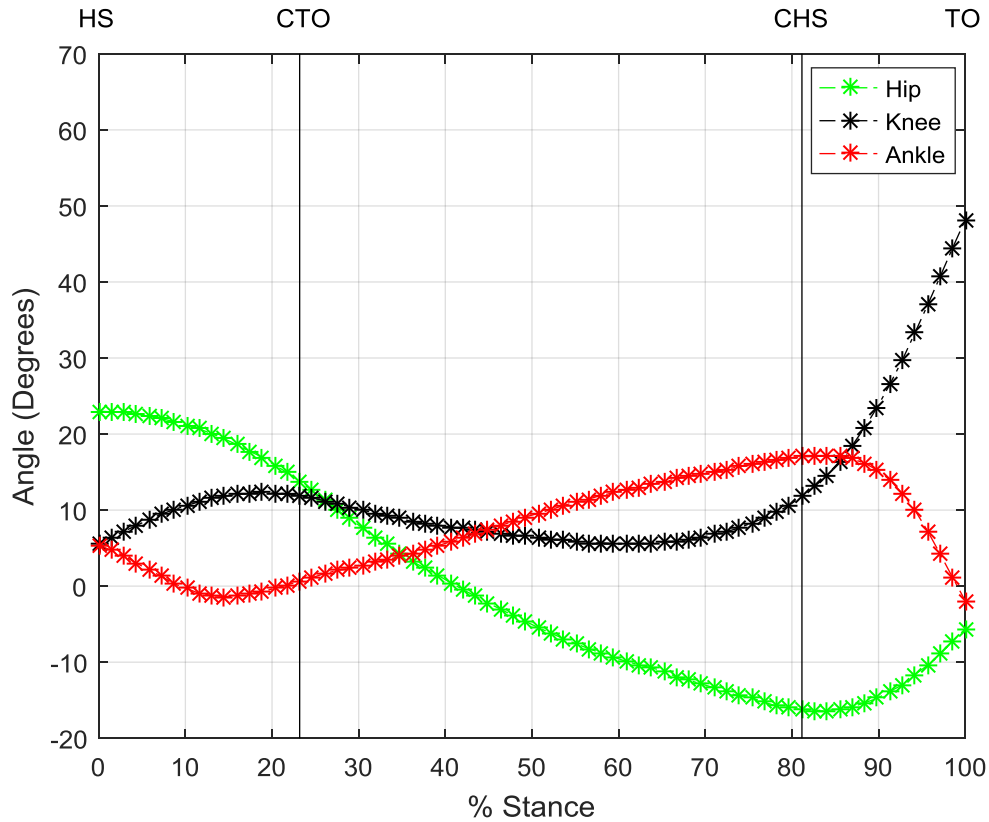


Figure 15: Joint angles for the leg during the walking exercise beginning with heel strike

5.1.3 Moments

Joint torque data for the stance phase of gait is presented in this section. Specifically, these are flexion/extensor moments for the hip, knee, and ankle. The results obtained from an inverse dynamics based approach for the motion of walking match very well with other previously reported investigations into joint moments (Winter 2009; Browning & Kram, 2007; Neptune et al., 2001; John et al., 2012). For all of these results, the values on the ordinate axes were normalized with respect to body mass. This means that their values were in units of Newton-meters per kilogram. Additionally, these figures include vertical bars which indicate the

following events during the gait cycle: heel strike (HS), contralateral toe-off (CTO), contralateral heel-strike (CHS), and lastly, toe-off (TO), as seen in **Fig. 2**, and used also in **Fig. 14** and **Fig. 15**. Finally, the color scheme for each comparison is consistent through the hip, knee, and ankle joint torque representations.

5.1.3.1 Hip. The hip joint torque data tended to have a large extensor peak initially, sometime before contralateral toe-off, between 0.5 and 1 N-m/kg (**Fig. 16**). Throughout the

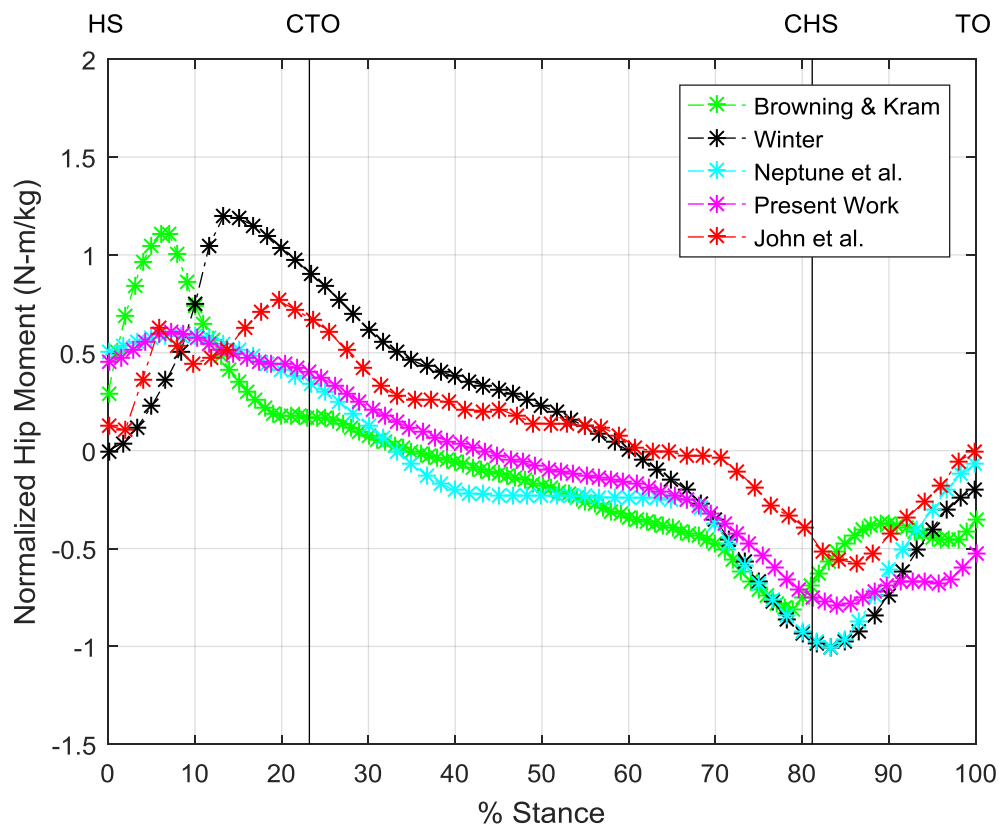


Figure 16: Joint moments in the hip during walking

progression of stance however, the hip moment decreases, indicating there is a flexor moment towards the end of stance. The hip moment is the most variable in the lower-limb because it is responsible for a significant amount of stability for the upper body (Winter and Seinko, 1988).

5.1.3.2 Knee. Torque data for the knee during walking is presented in **Fig. 17**. The largest peak occurs very close to contralateral toe-off. During this extensor moment, the limb is loaded in such a way as to prevent collapse of the limb. The knee tends towards a flexor moment near contralateral heel strike, as the body is thrust forward during progression. Right before toe-off, the torque increases again, to a magnitude comparable to the one seen earlier in stance.

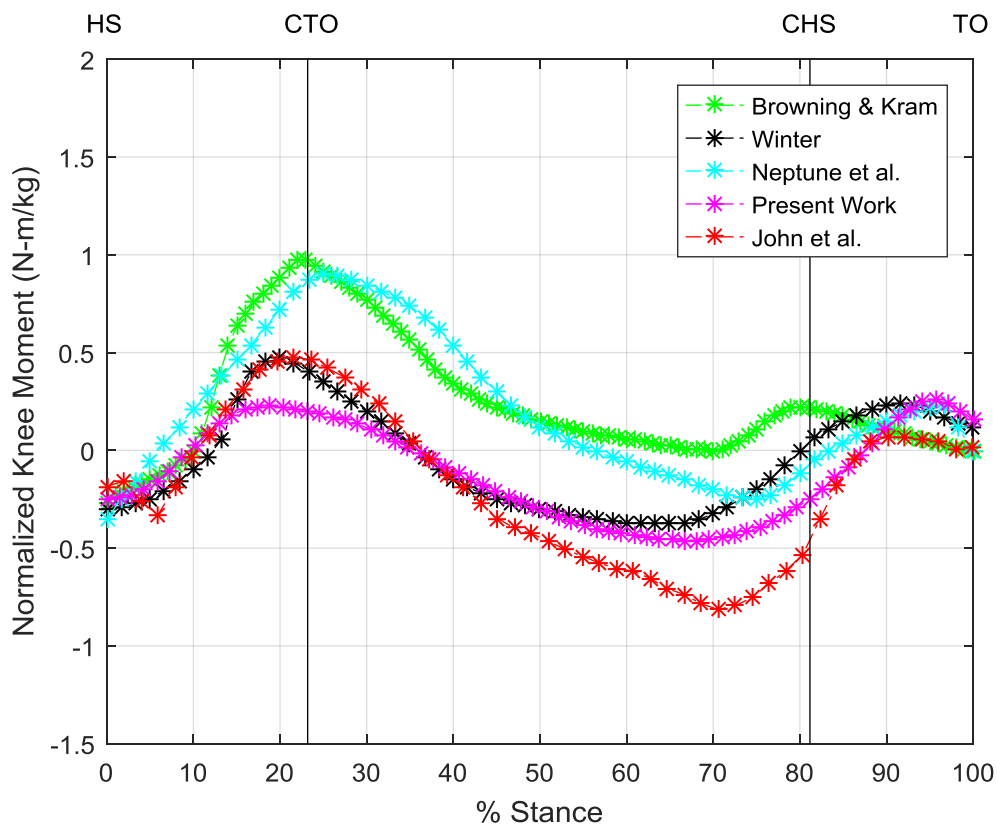


Figure 17: Joint moments in the knee during walking

5.1.3.3 Ankle. Lastly, torque data for the ankle joint during the stance phase of gait is presented in **Fig. 18**. A small, dorsiflexion moment was observed, approximately 20 N-m/kg during walking. This matched well with other reported findings. It occurred prior to contralateral

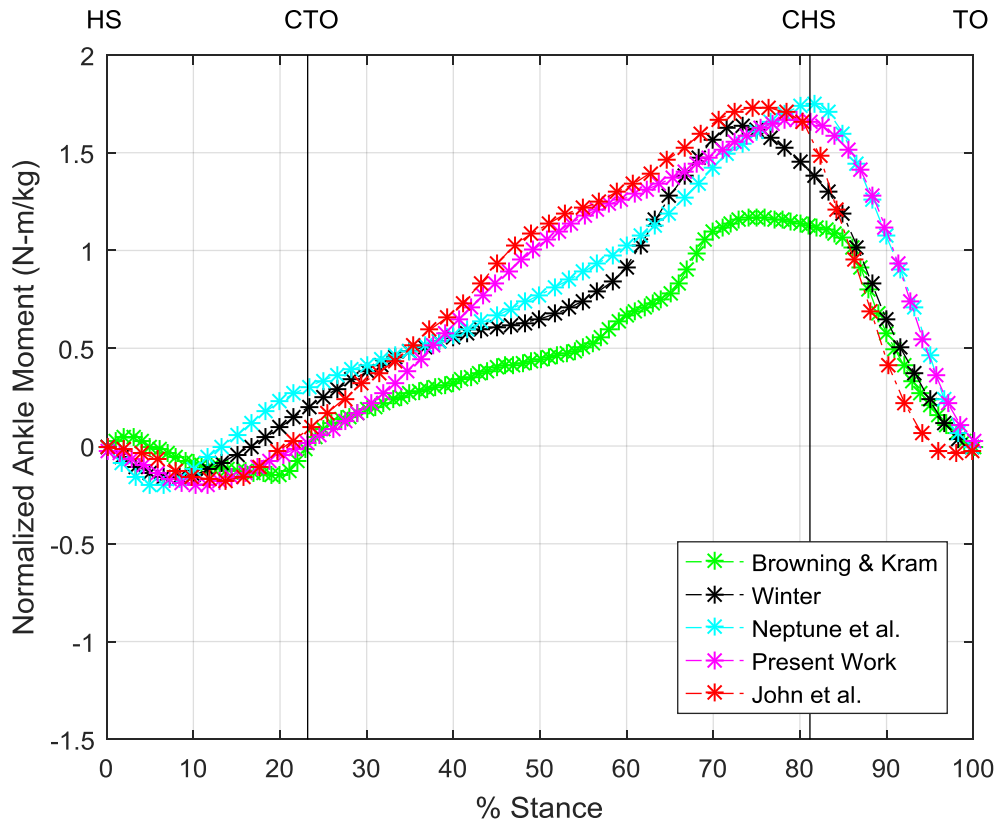


Figure 18: Joint moments in the ankle during walking

toe off. This exists such that the foot does not rotate too quickly after heel strike. A large plantar flexion moment occurs near contralateral heel strike, which represents the effort needed to produce push off.

5.1.4 Muscle Force Estimations

Muscle force estimations were made following an inverse dynamics based approach. The primary muscle groups that contribute to locomotion in the thigh are seen in **Fig. 19**. Presented are the follow muscle groups: the iliopsoas, rectus femoris, hamstrings (including the semimembranosus, semitendinosus, biceps femoris longhead, and biceps femoris shorthead), vastus lateralis, gluteus maximum, and gluteus medius. The figure displays gait beginning with heel strike and ending with toe-off. Various events for gait are included for reference.

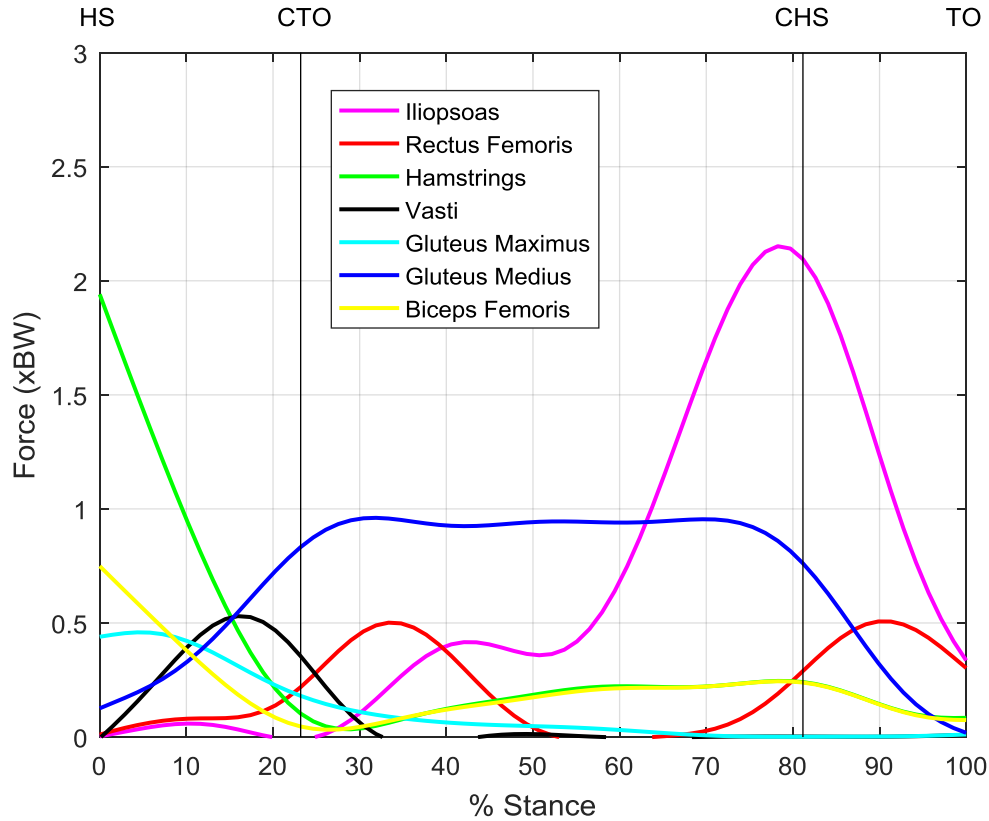


Figure 19: Force estimation in the thigh during stance

Similarly, muscle force estimations for the shank are seen in **Fig. 20**. The primary contributors that were examined were the gastrocnemius and the soleus.

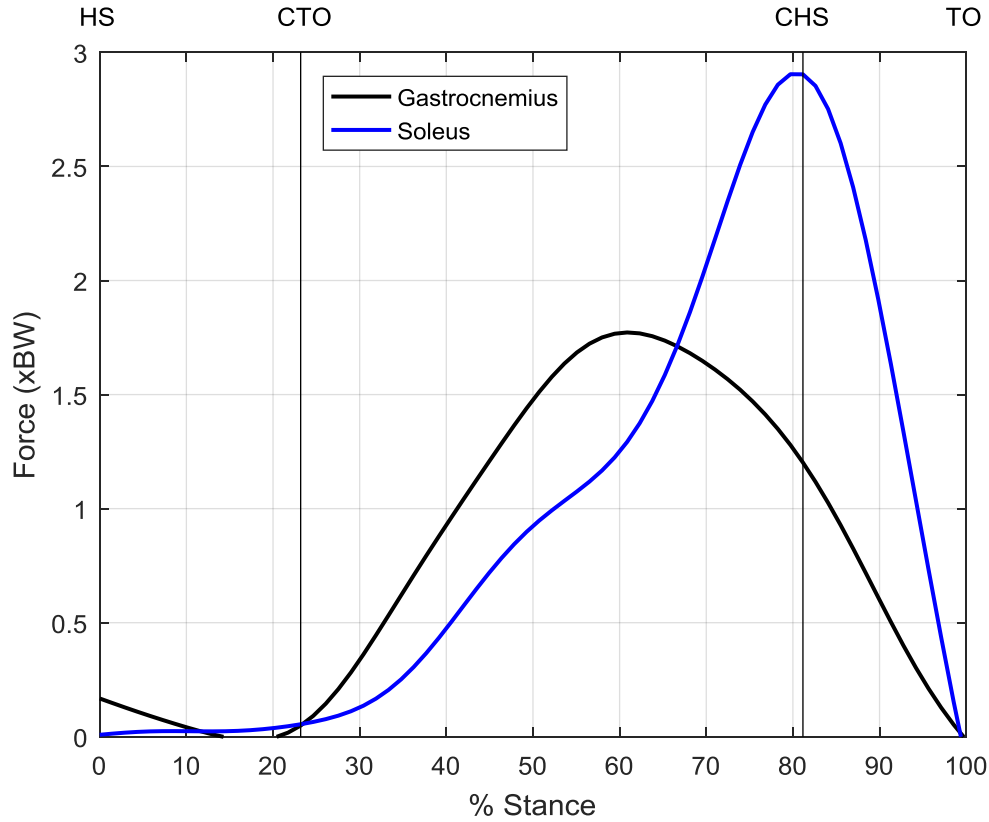


Figure 20: Force estimation in the shank during stance

Muscle contributions for gait in the lower extremity was compared with Pandy & Andriacchi (2010). These comparisons are displayed in **Fig. 21**. Red lines indicate the muscle force estimations for the present work. The follow functional muscle groups were compared: (A) gastrocnemius, (B) iliopsoas, (C) the vasti (comprised of the vastus lateralis, vastus intermedialis, and vastus medialis), (D) rectus femoris, (E) hamstrings (comprised of the semimembranosus, semitendinosus, biceps femoris long head, and biceps femoris short head), and (F) gluteus

maximus. Please see Appendix A with regards to the muscles themselves indicated in the 2392 OpenSim model.

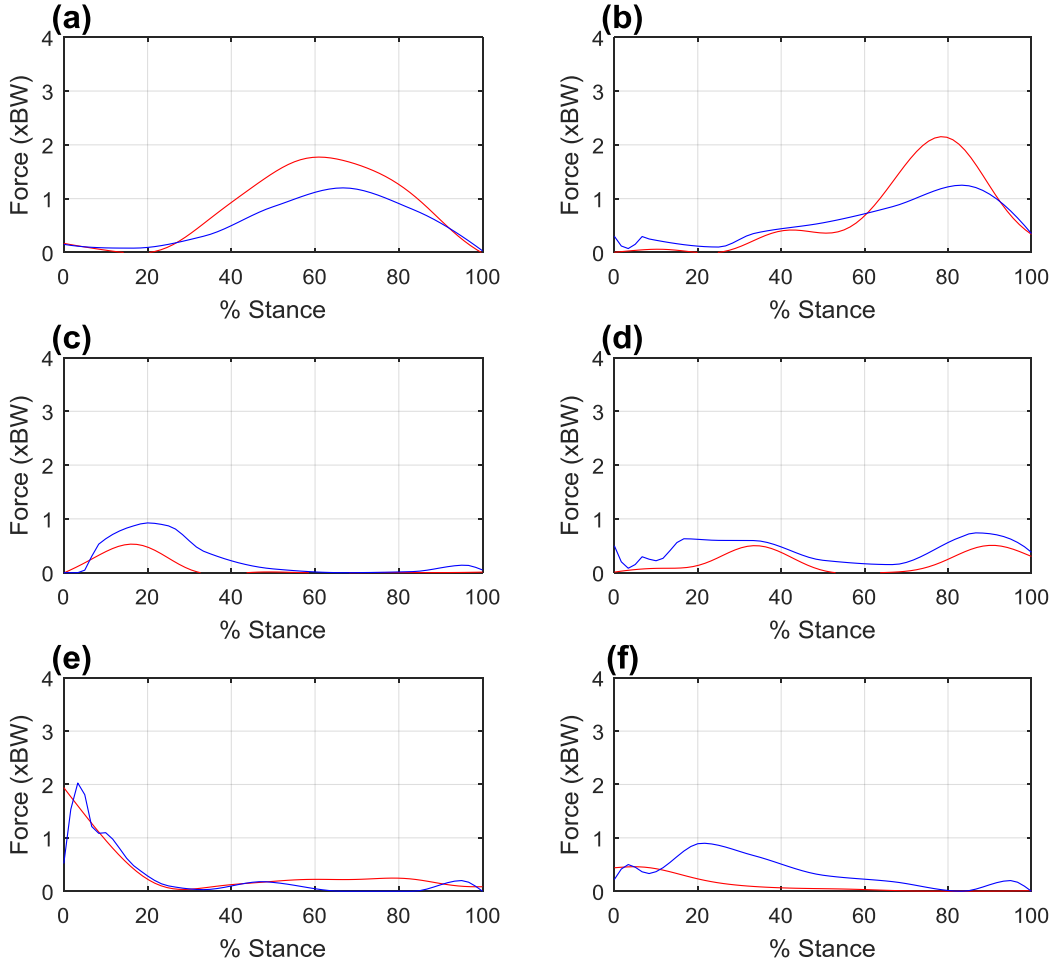


Figure 21: Force estimations compared with Pandy & Andriacchi (2010)

5.1.5 Joint Reaction Forces

Inter-segmental loads were collected and were compared with previous reports (Seireg & Arkivar, 1975; Morrison, 1970; Hardt, 1978; Crowninshield & Brand, 1981; Glitsch &

Baumann, 1981; Collins, 1995; Brand et al., 1994; Anderson & Pandy, 2001; Pandy & Andriacchi, 2013). Peak values for loading at the hip, knee, and ankle joint reaction force during stance can be seen in **Figs. 22, 23, and 24**, respectively.

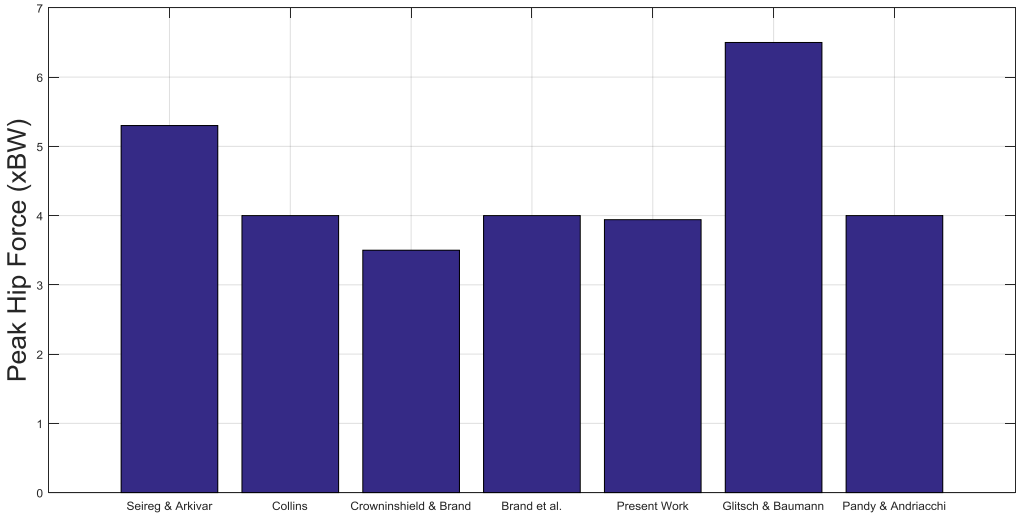


Figure 22: Peak loading at the hip joint during gait

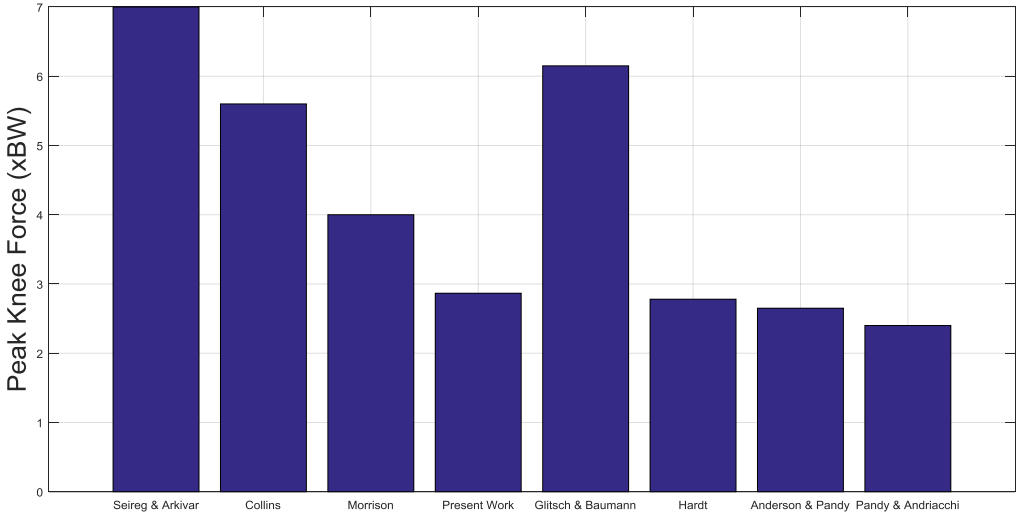


Figure 23: Peak loading at the knee joint during gait

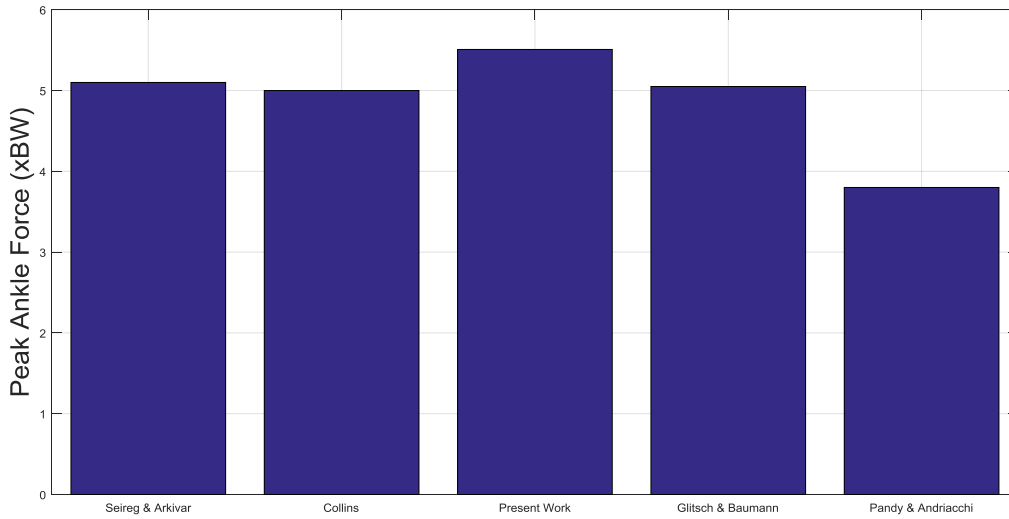


Figure 24: Peak loading at the ankle joint during gait

5.2 Biomechanics of Golf

5.2.1 Trailing vs. Leading Leg GRFs

The ground reaction forces in both legs were captured and are of significance. Unlike gait, the motion of the golf swing is asymmetric. Accordingly, a variation in the reaction forces between the leading and trailing leg in the vertical direction is seen in **Fig. 25**. The dynamic events described for **Fig. 5** are represented in **Fig. 25**. The distribution of weight at address is impacted by stance. For this particular case, the leading leg held slightly more weight than the trailing leg at address. As the motion of the swing progresses, weight is shifted from the leading leg to the trailing leg in order to drive the club through impact. During follow-through, weight is transferred back to the leading leg.

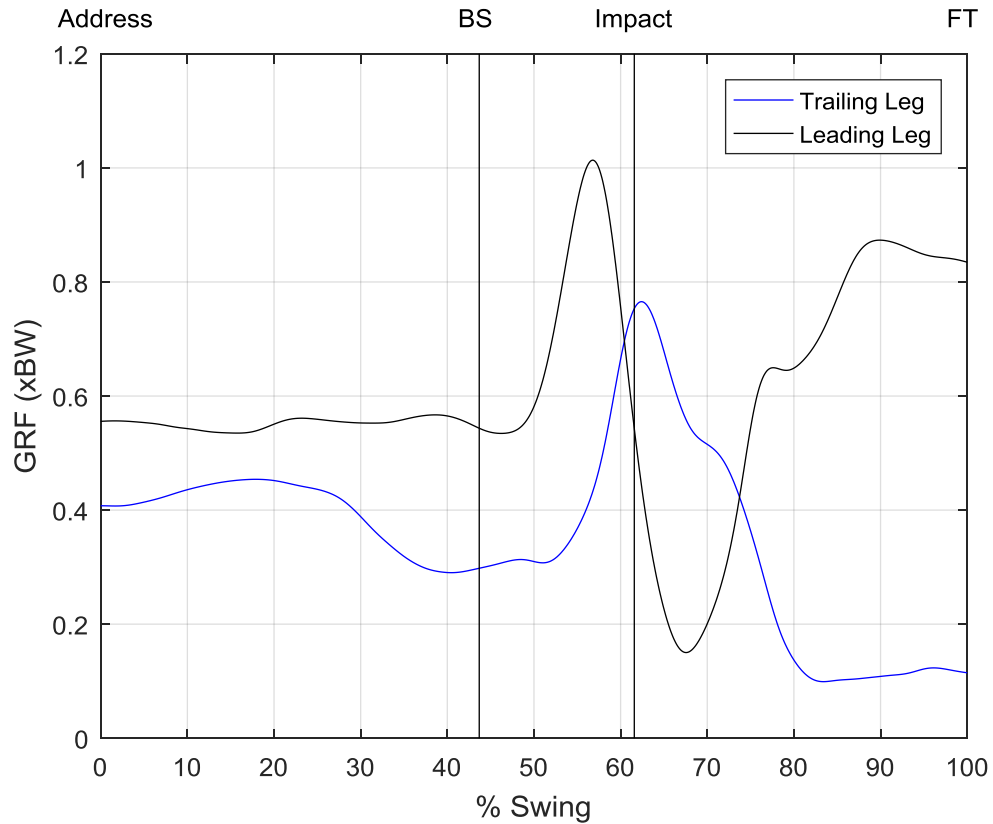


Figure 25: Ground reaction force data in the vertical direction during the golf swing

The trailing leg ground reaction force data is seen in **Fig. 26**. Similar to gait, this force was broken down into three reaction components, R_x , R_y , and R_z , which represent the medio-lateral, proximal-distal, and anterior-posterior directions, respectively. It is not surprising that a large vertical (proximal-distal) reaction force is observed. A medially directed reaction force is present from address to follow-through, with a peak near impact. An anteriorly directed force is present prior to impact, with a peak of 17% BW seen near the top of the backswing.

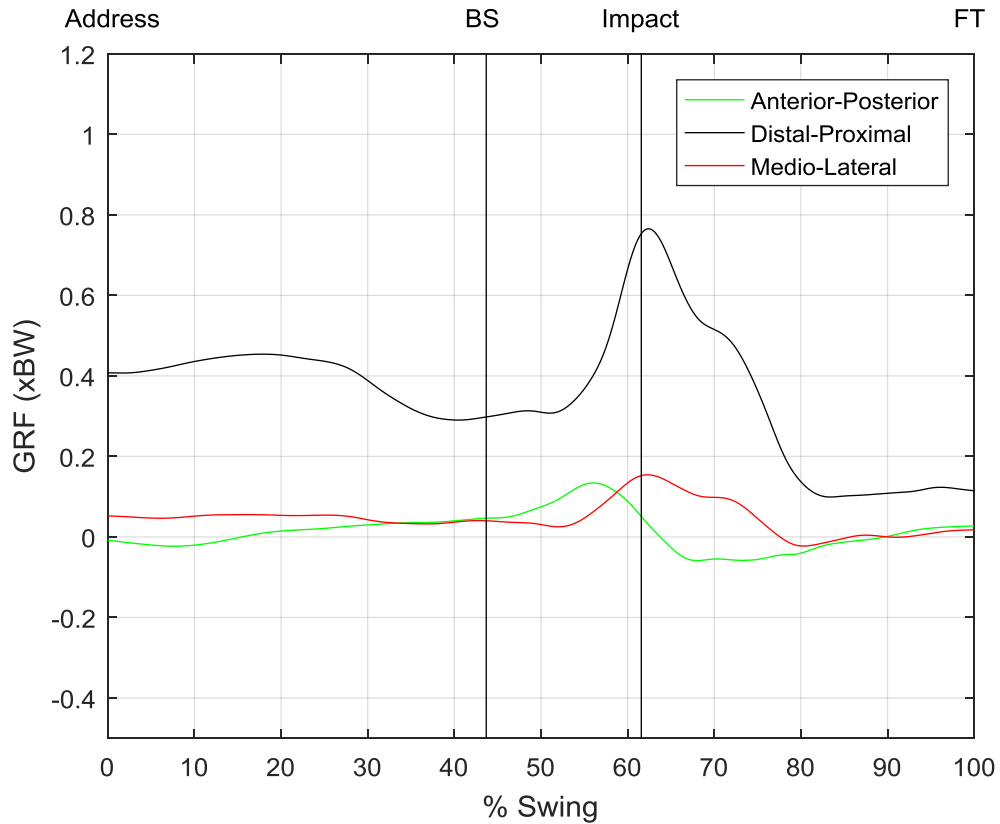


Figure 26: Ground reaction force data in the trailing leg during the golf swing

The leading leg ground reaction force data is seen in **Fig. 27**. Similar to the trailing leg, the vertical, or proximal-distal, reaction force was the largest. A subtle laterally directed reaction force was observed, in addition to a small posteriorly directed reaction force. The vertical reaction force approaches, or is near, a minimum at impact.

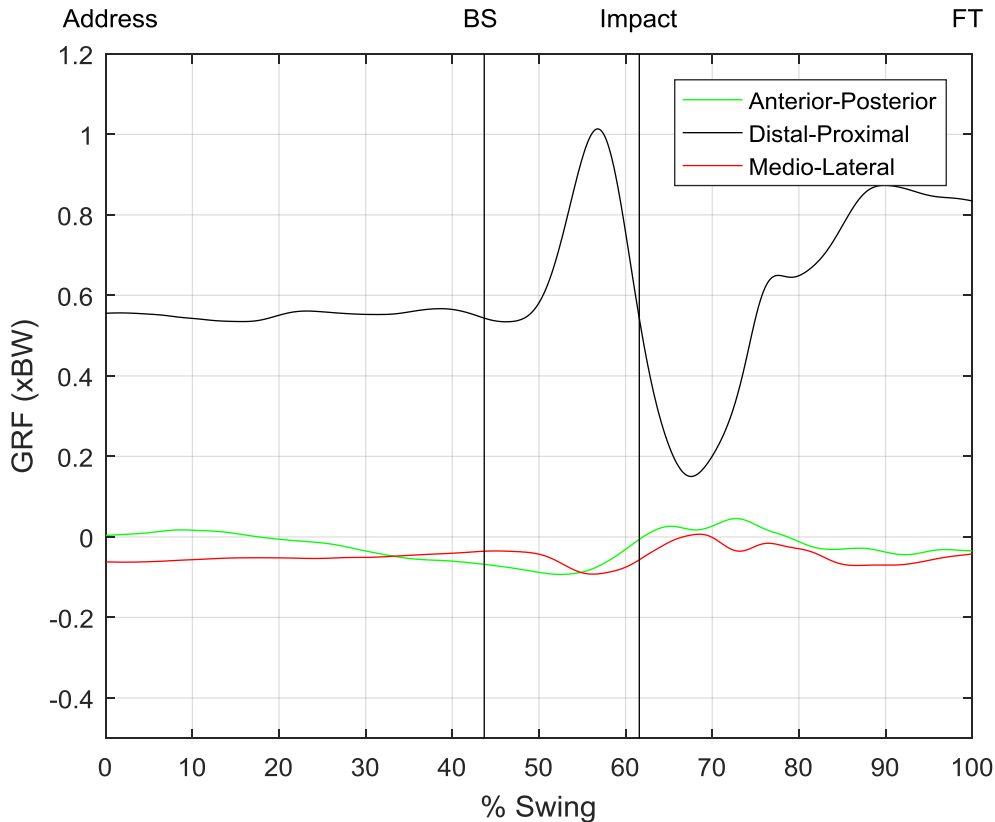


Figure 27: Ground reaction force data in the leading leg during the golf swing

5.2.2 Trailing vs. Leading Leg Joint Angles

Knee flexion angle during the golf swing for both legs was obtained and can be seen in **Fig. 28**. This figure displays the timing of the knee kinematics relative to impact on the abscissa. At address, flexion in both knees was very similar, between approximately 30-35°. The trailing knee decreased in flexion slightly during the backswing, but increased thereafter, reaching a final flexion angle of approximately 45°. The leading leg experienced a gradual decrease in knee flexion angle throughout the swing, terminating near 15° flexion.

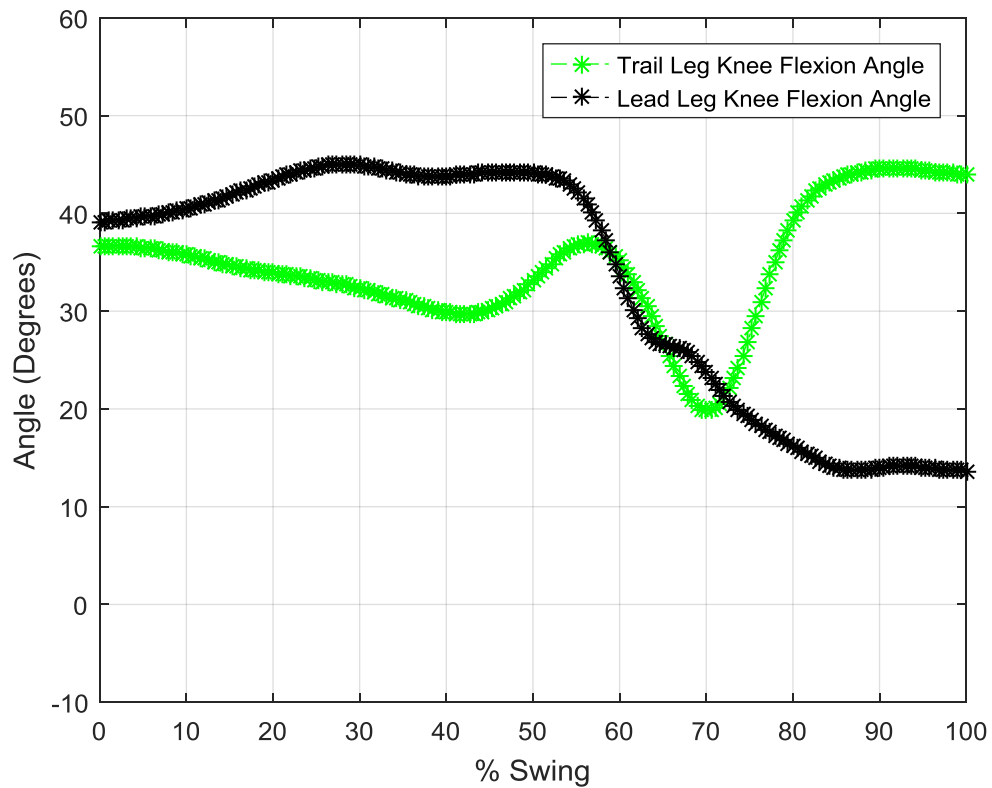


Figure 28: Leading and trailing knee flexion angles during the golf swing

5.2.3 Moments

5.2.3.1 Hip. Figs. 29 and 30 indicate the hip joint moments for each plane during the golf swing for the trailing leg and leading leg, respectively. These results were compared with Foxworth et al. (2013) in Figs. 31-36 for each plane in each leg. The shaded areas in the graphs for Foxworth et al. (2013) represent average values for hip joint moments \pm one standard deviation.

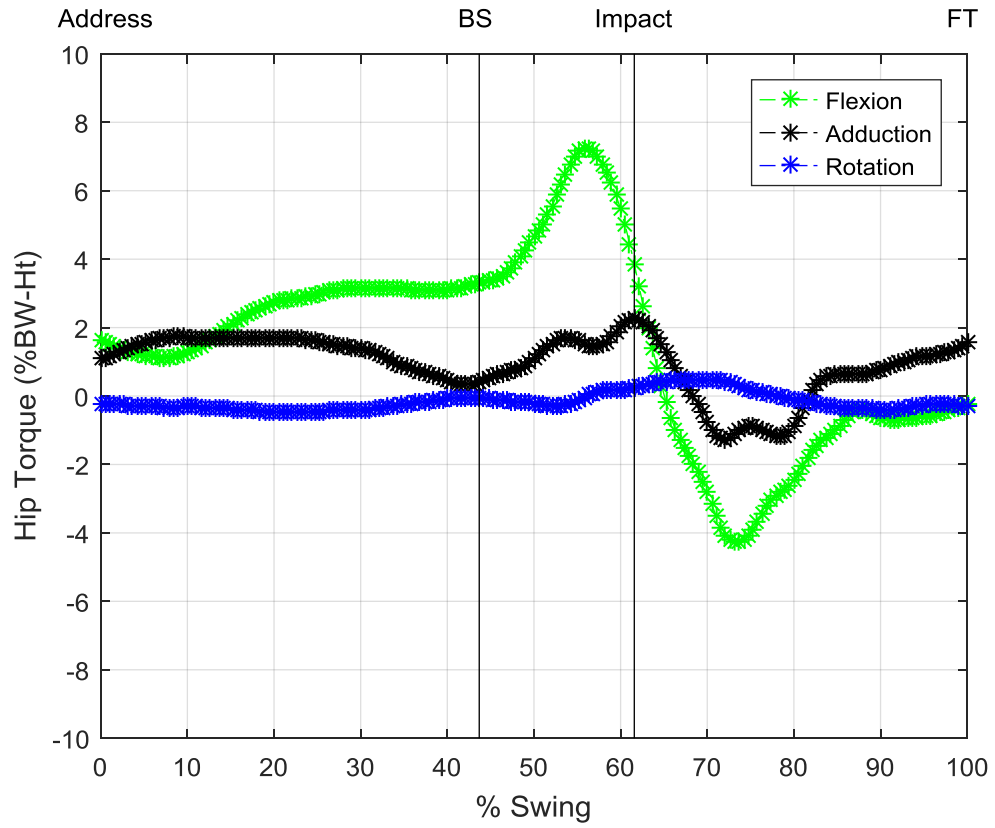


Figure 29: Joint torque data in the trailing leg hip during the golf swing

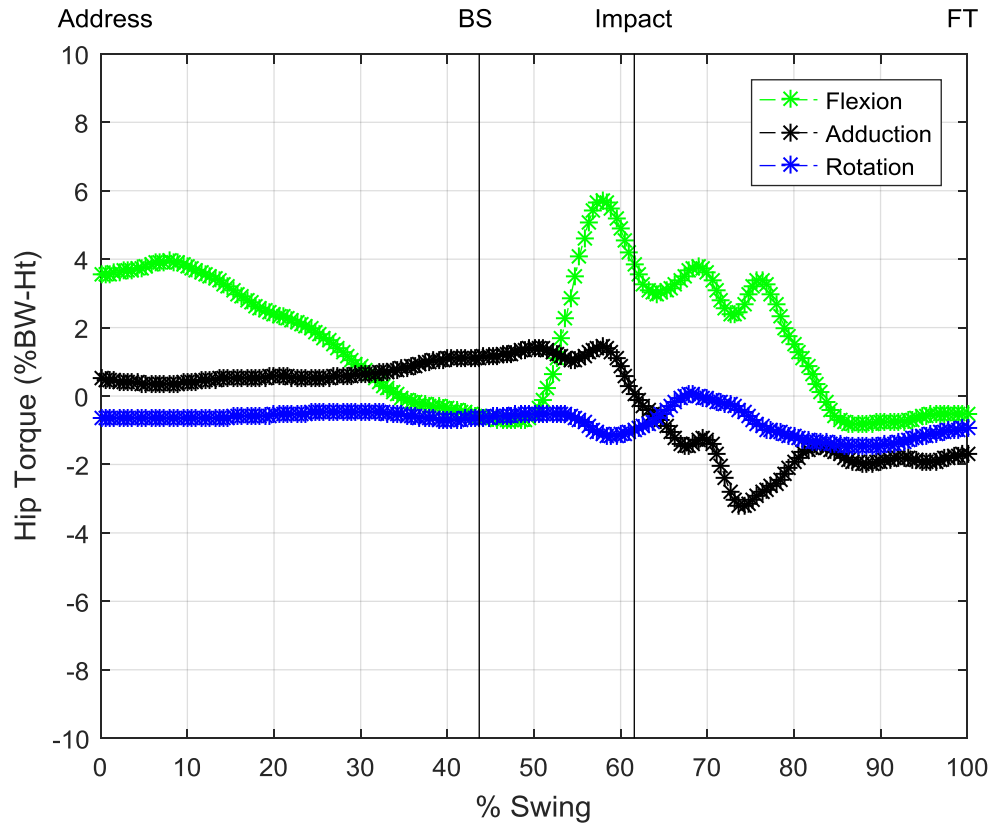


Figure 30: Joint torque data in the leading leg hip during the golf swing

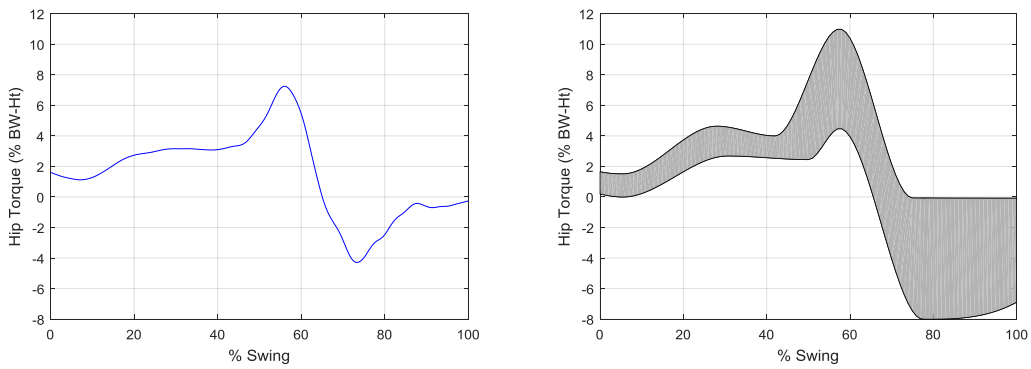


Figure 31: Hip extensor moments for the trailing leg with comparison

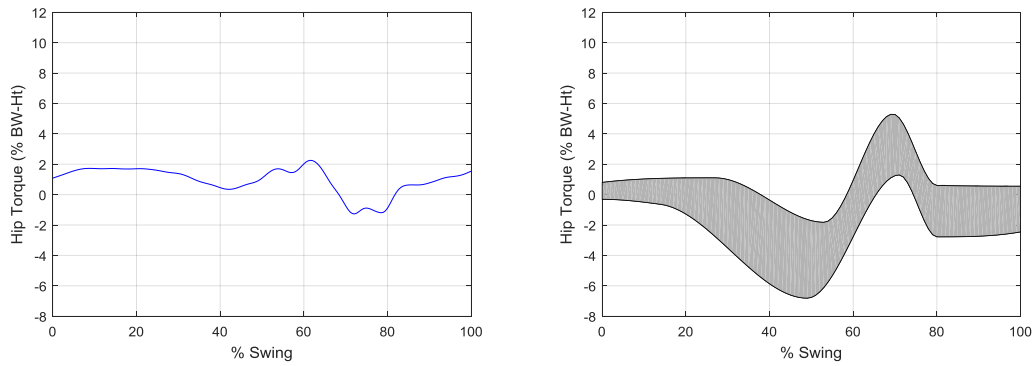


Figure 32: Hip adduction moments for the trailing leg with comparison

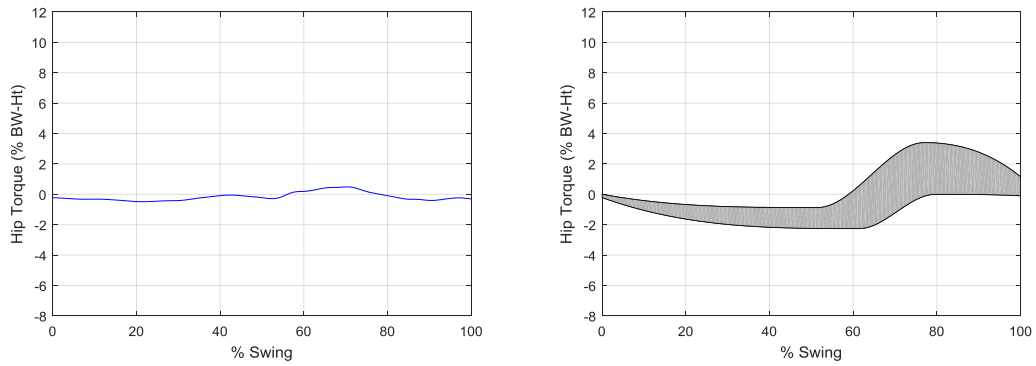


Figure 33: Hip internal rotation moments for the trailing leg with comparison

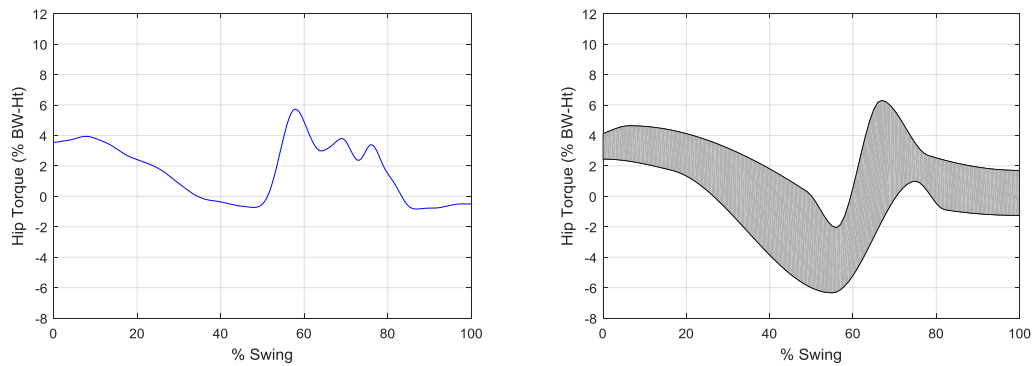


Figure 34: Hip extensor moments for the leading leg with comparison

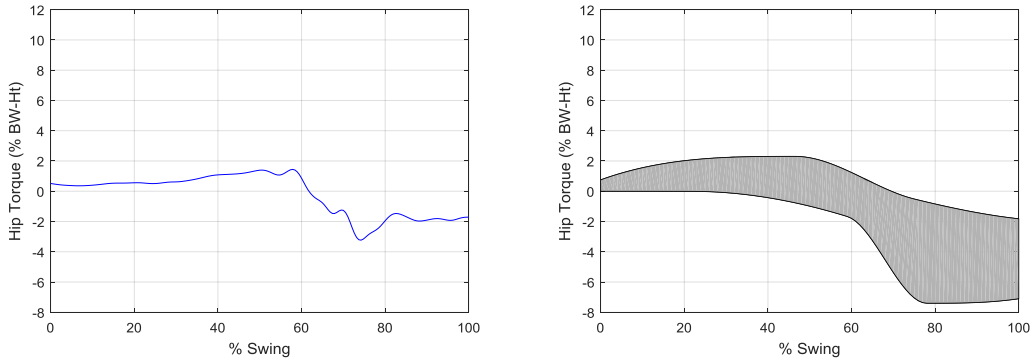


Figure 35: Hip adduction moments for the leading leg with comparison

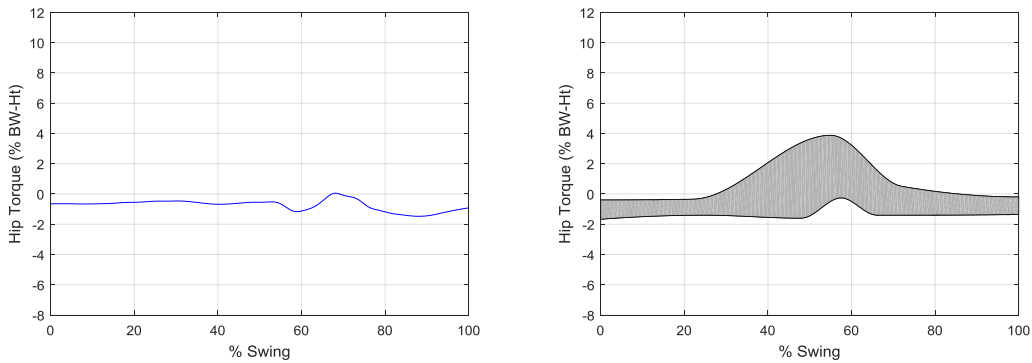


Figure 36: Hip internal rotation moments for the leading leg with comparison

5.2.3.2 Knee. Knee flexion moments can be seen in **Fig. 37**. Calculations were normalized (Moisio et al., 2003). A positive flexion moment for the trailing leg was observed prior to impact, with a peak value reaching approximately 3% BW-Ht. An increase in extensor moment was observed shortly thereafter through impact and follow-through. The leading leg experienced a peak extensor moment during the downswing, as the limb prepared for contact. Then, at impact, a peak flexion moment was observed in the leading leg was observed, which dissipated during follow-through.

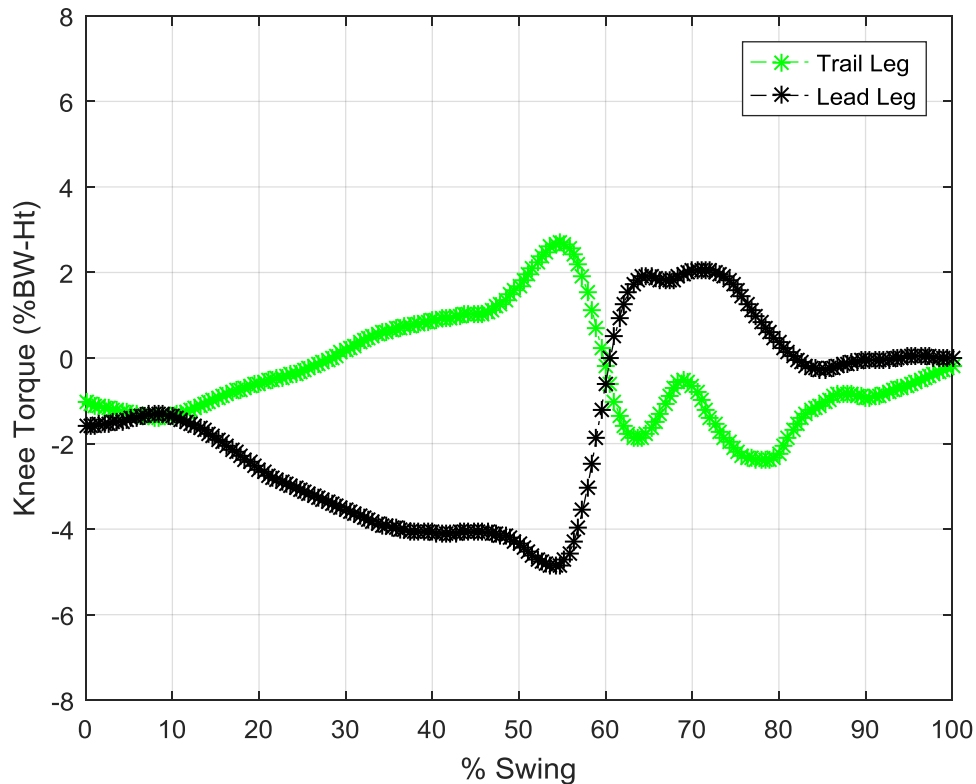


Figure 37: Joint torque in the knees during the golf swing

5.2.4 Muscle Force Estimations

Muscle force estimations can be seen in **Figs. 38** and **39**. Throughout the golf swing, muscle contribution to motion was analyzed independently for each leg. While the musculoskeletal model generated predictions for all 92 muscles used in the model, only muscles of interest were presented which include but are not limited to: biceps femoris, rectus femoris, gastrocnemius, vastus lateralis, gluteus medius & maximum, & semimembranosus. Estimates for muscle force generation were reasonable, with estimates for various muscles ranging from 250 – 1500 N. In the figures presented, the various phases of the golf swing is presented, including:

address, top of backswing (BS), impact, and end of follow-through (FT). A majority of the activation of the muscles presented occurred during follow-through, primarily because that is when motion in the lower-limb occurred for the golf swing. To the best of our knowledge, no reports on muscular force have been reported for the lower extremities during the golf swing, which suggest novelty for the current work.

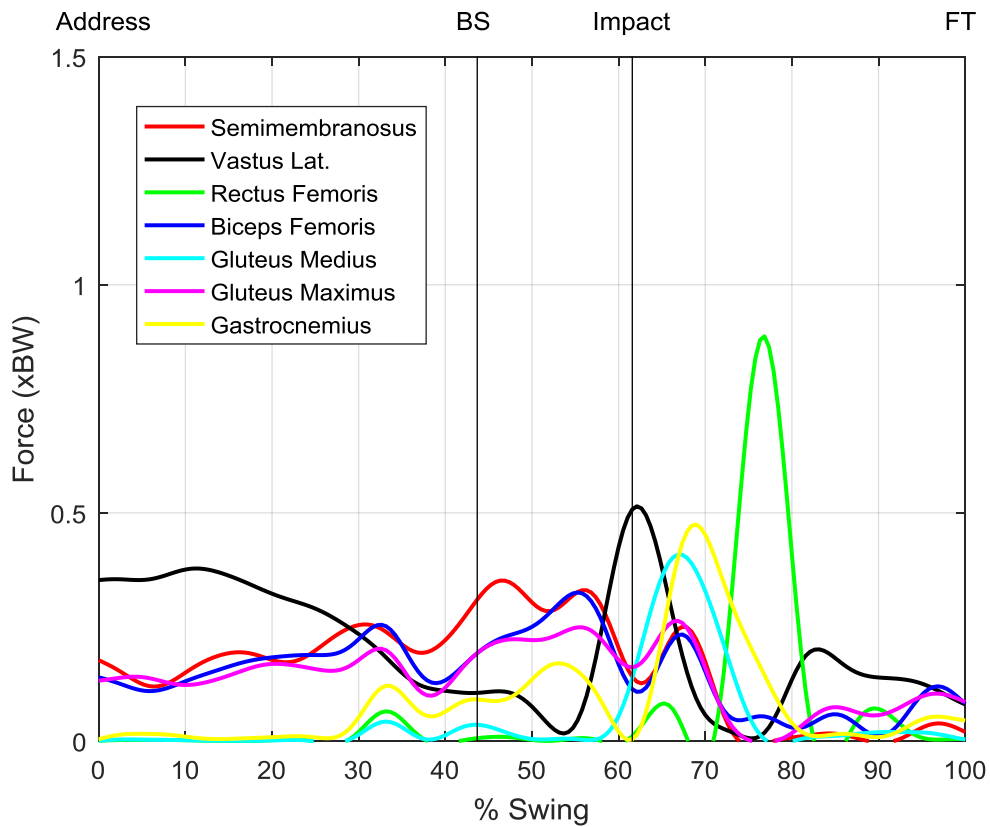


Figure 38: Force estimation in the trailing leg during the golf swing

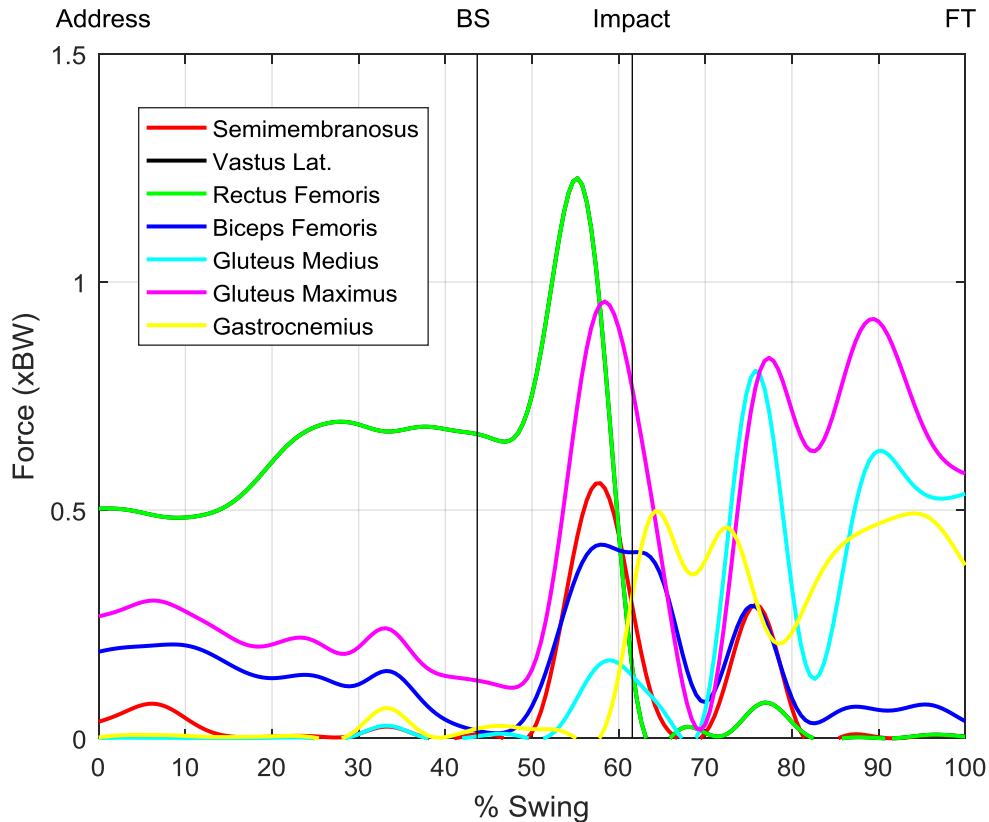


Figure 39: Force estimation in the leading leg during the golf swing

5.2.5 Joint Reaction Forces

Additionally, joint kinetics indicate that the joints experience loading differently. Peak hip loading was approximately 3x BW and peak knee joint loading was 4x BW, which can be seen in **Fig. 40** and **41** respectively. It is worthwhile to note that these loads represent the resultant sum at each joint and are explicitly different from contact forces. **Fig. 42** and **43** report these peak values and those obtained from other reports (D’Lima et al., 2008; Mündermann et al., 2008; Gatt et al., 1998). The former two reports, indicated by a single asterisk (*) indicate

that these values were obtained from an instrumented prosthetic, and not from an inverse dynamics based approach, which is indicated by a double asterisk (**).

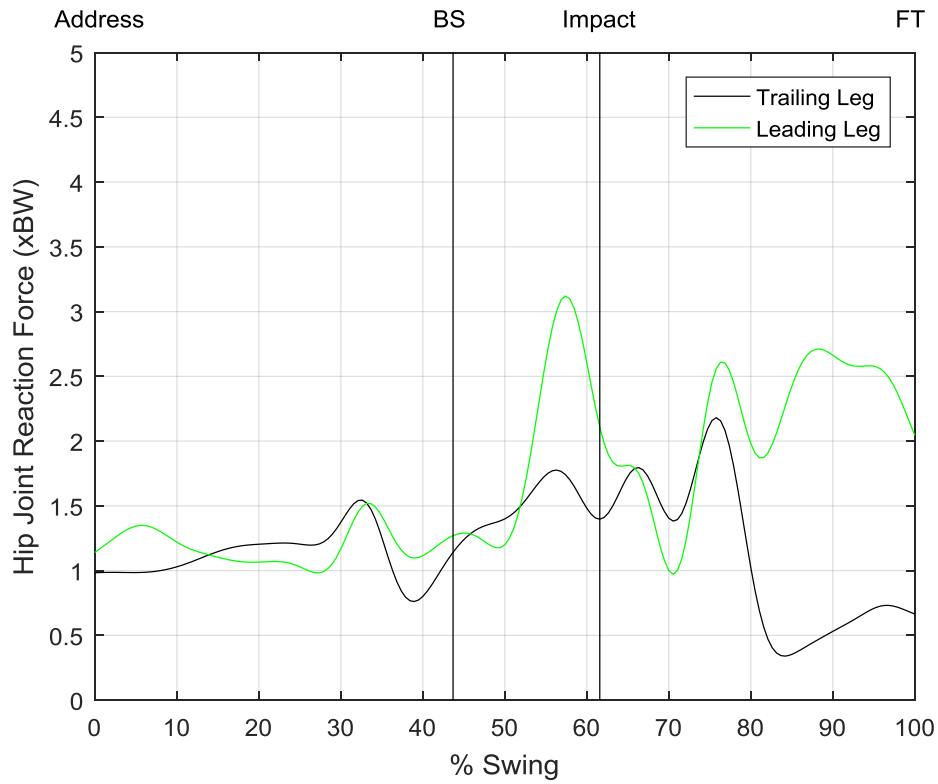


Figure 40: Loading at the hip joint during the golf swing

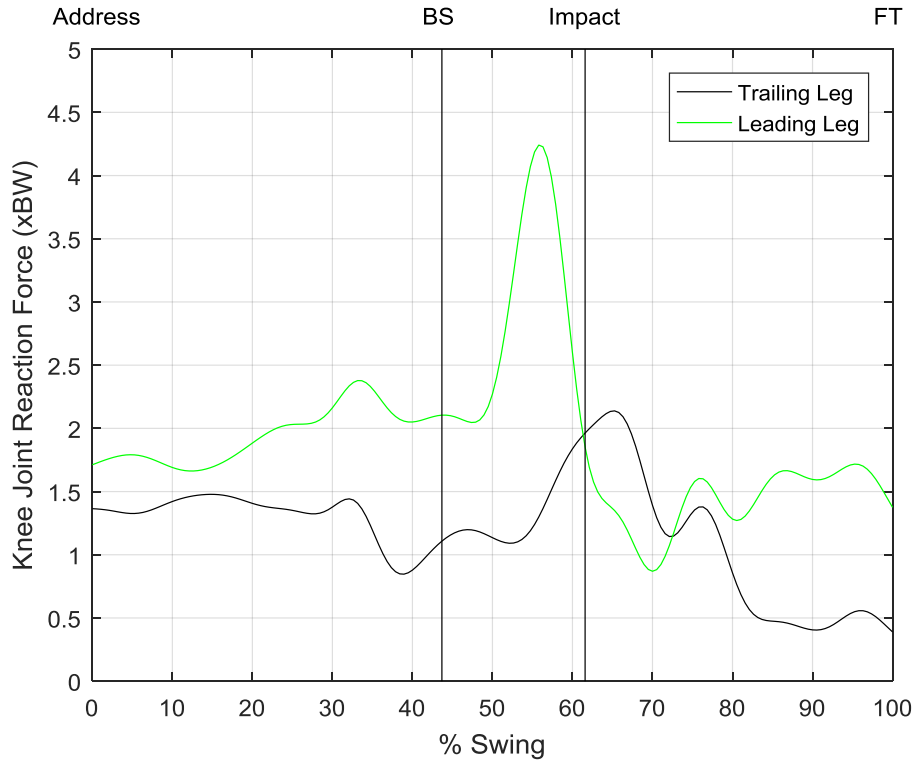


Figure 41: Loading at the knee joint during the golf swing

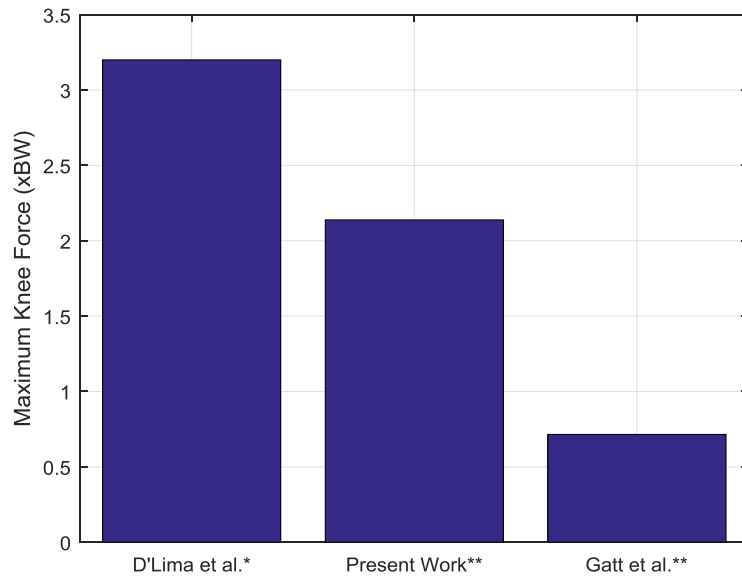


Figure 42: Peak loading in the trailing knee during the golf swing

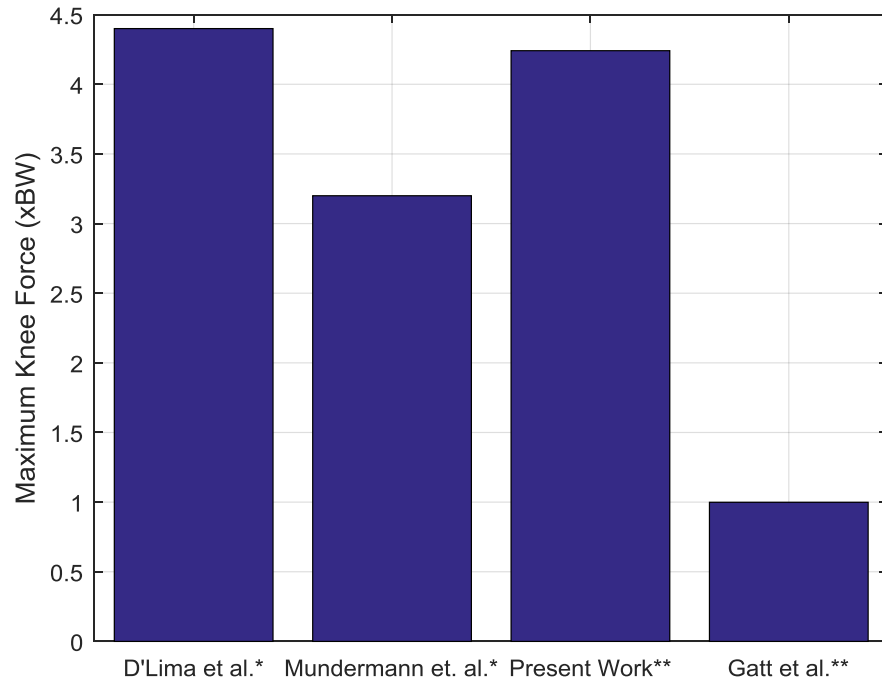


Figure 43: Peak loading in the leading knee during the golf swing

CHAPTER VI

DISCUSSION

6.1 Conclusions from Motion Studies

The sagittal plane knee kinematics for the golf swing typically correlated well with previous observations (Gatt et al., 1998; Pfeiffer et al., 2014; Choi et al., 2015). All studies, including the present work, indicate that at address, both knees are initially flexed at very similar angles. As the golf swing motion progresses, the terminating lead knee flexion angle is substantially lower than the trailing leg lead knee. This is not surprising, considering the inherent motion of the golf swing.

Comparisons regarding knee flexion moments were made with other studies. Peak flexion moments were observed in the lead leg at impact which is similar to other studies (Gatt et al., 1998; Choi et al., 2015). This occurs primarily because of the shift in weight towards the trail leg near impact. Another similarity with previous investigations was the trailing leg knee joint moment. Peak flexion moment values were observed near impact. In order to drive the club through impact, a shift in weight towards the trailing leg results in a tendency for the shank to be rotated ventrally with respect to the thigh.

Overall, the hip joint torques are in strong agreement with other work (Foxworth et al., 2013). In **Fig. 31**, the trailing limb reaches a peak hip extensor moment, between 6-12 % BW-Ht during the downswing. A peak flexion moment is observed following impact. These

values are not dissimilar from the torques displayed during walking (Winter, 2005) This supports the notion that golf is a low risk exercise for rehabilitation programs.

Conclusions can be made using inverse dynamics to estimate muscle force generation and joint loading during the golf swing. Force estimations from **Figs. 38 & 39** in both legs indicate activations at different points during the golf swing. These can be compared with EMG recordings, which offer insight into muscular activity only. To our best knowledge, only a few investigations have reported muscular activity for the lower extremities during the golf swing. Bechler et al. (1995) focused specifically on the hip and knee, while McHardy & Pollard (2005) reported muscle activations in the upper body and some in the lower body. Activity for the semimembranosus for both legs match that with Bechler et al. Activations in the trailing and leading legs were highest during the downswing and near impact, respectively. Similarly, the vastus lateralis and gluteus maximus activation in the leading leg matches Bechler et al., with the latter matching McHardy & Pollard as well. Some results matched McHardy & Pollard but not Bechler et al. For example, the gluteus medius activations in the trailing leg from McHardy & Pollard's study matched the present work but not Bechler et al. And the vastus lateralis for the trailing leg did not match Bechler et al., though there was a large variation reported by phase for this muscle. Accordingly, there are some similarities and differences for selected muscles with these studies. This is a subtle difference from, for example, skill level, which was determined not to confound results previously (Gatt et al., 1998). To the best of our knowledge , there are no investigations using inverse dynamics to understand technique variations in the golf swing.

The leading leg experienced more joint loading than the trailing leg at both the hip and knee joints, as seen in **Fig. 40** and **41**. This could be due to the recovery of posture following

impact. These values are explicitly similar to predicted values for gait, indicating that prosthetic failure due to fatigue for the golf swing is comparable to gait.

6.2 Limitations of Current Work

There were several limitations of the current work. First, the approach to estimate kinematic and kinetic information was driven by an inverse dynamics approach, which is prone to error that occurs during experimentation. Investigations that use muscle-driven simulations to analyze motion have shown to reduce this error, indicating that they are indeed more accurate. This approach, a forward dynamics analysis, was determined to be excluded from the investigation because of scope; this investigation is purely inverse dynamics. Another limitation was technical by nature. The present work makes no considerations for ligaments. The investigation was primarily driven to use OpenSim at a high-level, and avoid low-level implementation using C/C++. Incorporating ligaments in the musculoskeletal model would require writing plugins in C/C++. Another limitation of the investigation was institutional by nature. The ability to compare and analyze information not only from inverse dynamics, but potentially from instrumented prosthetics, such as in Brand et al. (1994), can yield high value. Additionally, only one participant was analyzed. Having a larger sample size would have increased robustness for the investigation. Lastly, the marker set itself yielded a small limitation. And while error reduction during scaling was performed to increase accuracy (Hicks et al., 2015), incorporating a larger marker set may have had positive consequences.

6.3 Clinical Recommendations

This work aimed to provide objective evidence regarding the safety of the golf swing as a rehabilitation exercise. Inverse dynamics was used to compute kinetic and kinematic information for both legs. Care was taken in the approach and execution during method formulation and experimentation. Multiple investigations on the biomechanics of the lower-limb have already reported no significant influence is made regarding shoe type, age, or skill level regarding the biomechanics of the lower-limb (Gatt et al., 1998; Foxworth et al., 2013).

With respect to joint replacements, there is no golden rule or definitive characteristic that excludes an exercise from a rehabilitation program. The clinical formulation behind a regimented program is most nearly subjective by nature. There does however seem to be standard consensus regarding the level of impact, i.e. joint loading, that should be tolerated (Kuster, 2002; Swanson et al., 2009). Typically, the exercises that are most suited for a rehabilitation regimen constitute activities that limit high impact loading, which can accelerate wear or compromise fixation in TKR patients (Andriacchi & Hurwitz, 1997). Ultimately however, rehabilitation program development should be customized to individual patients, with objective evidence serving as a resource to that end.

REFERENCES

- Anderson, F., & Pandy, M., 2001b. "Static and dynamic optimization solutions for gait are practically equivalent," *Journal of Biomechanics*, Vol. 34, pp. 153-161.
- Andriacchi, T.P., Hurwitz, D.E., 1997. "Gait biomechanics and the evolution of total joint replacement," *Gait and Posture*. Vol. 5, pp. 256-264.
- Baker, M.L., Epari, D.R., Lorenzetti, S., Sayers, M., Boutellier, U., Taylor, W.R., 2017. "Risk factors for knee injury in golf: a systematic review," *Sports Medicine*. Vol. 47, pp. 2621-2639.
- Barre, A., Armand, S., 2014. "Biomechanical ToolKit: Open-source framework to visualize and process biomechanical data," *Computer Method and Program in Biomedicine*, Vol. 114, pp. 80-87.
- Bechler, J.R., Jobe, F.W., Pink, M., Perry, J., Ruwe, P.A., 1995. "Electromyographic analysis of the hip and knee during the golf swing," *Clinical Journal of Sports Medicine*. Vol. 5, pp. 162-166.
- Brand, R.A., Pederson, D.R., Davy, D.T., Kotzar, G.M., Heiple, K.G., Goldberg, V.M., 1994. "Comparison of hip force calculations and measurements in the same patient," *The Journal of Arthroplasty*. Vol. 9, pp. 45-51.
- Browning, R., Kram, R., 2007. "Effects of obesity on the biomechanics of walking at different speeds," *Medicine & Science in Sports & Exercise*, Vol. 39, pp. 1632-1641.
- Choi, A., Sim, T., Hwan Mun, J., 2015. "Quasi-stiffness of the knee joint in flexion and extension during the golf swing," *Journal of Sports Sciences*. Vol. 33, pp. 1682-1691.
- Collins, J., 1995. "The redundant nature of locomotor optimization laws," *Journal of Biomechanics*, Vol. 28, pp. 251-267.
- Crowninshield, R., Brand, R., 1981. "A physiologically based criterion of muscle force prediction in locomotion," *Journal of Biomechanics*, Vol. 14, pp. 793-801.
- D'Lima, D.D., Steklov, N., Patil, S., Colwell Jr., C.W., 2008. "The Mark Coventry Award: In vivo knee forces during recreation and exercise after knee arthroplasty," *Clinical Orthopedic Related Research*. Vol. 466, pp. 2605-2611.

- Damsgaard, M., Rasmussen, J., Christensen, S., Surma, E., de Zee, M., 2006. "Analysis of musculoskeletal systems in the AnyBody Modeling System," *Simulation Modeling Practice and Theory*, Vol. 14, Iss. 8, pp. 1100-1111.
- Delp, S., Anderson, F., Arnold, A., Loan, P., Habib, A., John, C., Guendelman, E., & Thelen, D., 2007. "OpenSim: open-source software to create and analyze dynamic simulations of movement," *IEEE Transactions on Biomedical Engineering*, Vol. 54, Iss. 11, pp. 1940-1950.
- Delp, S.L., Loan, J.P., Hoy, M.G., Zajac, F.E., Topp, E.L., Rosen, J.M., 1990. "An interactive graphics-based model of the lower-extremity to study orthopaedic surgical procedures," *IEEE Transactions on Biomedical Engineering*. Vol. 37, pp. 757-767.
- Delp, S.L., Loan, J.P., 2000. "A computational framework for simulating and analyzing human and animal movement," *IEEE Computer Science & Engineering*. Vol. 2, pp. 46-55.
- Drillis, R., Contini, R., 1966. "Body segment parameters". Office of Vocational Rehabilitation, Department of Health, Education, And Welfare. New York, Rep. 1163-03.
- Erdemir, A., 2016. "Open Knee: open source modeling & simulation to enable scientific discovery and clinical care in knee biomechanics," *Journal of Knee Surgery*, Vol. 29, Iss. 2, pp. 107-116.
- Erdemir, A., McLean, S., Herzog, W., Bogert, A.J., 2007. "Model-based estimation of muscle forces exerted during movements," *Clinical Biomechanics*. Vol. 22, pp. 131-154.
- Foxworth, J.L., Millar, A.L., Long, B. L., Way, M., Vellucci, M.W., Vogler, J.D., 2013. "Hip joint torques during the golf swing of young and senior healthy males," *Journal of Orthopaedic & Sports Physical Therapy*. Vol. 43, pp. 660-665.
- Gatt, C.J., Pavol, M.J., Parker, R.D., Grabiner, M.D., 1998. "Three-dimensional knee joint kinetics during a golf swing," *The American Journal of Sports Medicine*. Vol. 26, pp. 285-294.
- Glitsch, U., Baumann, W., 1981. "The three-dimensional determination of internal loads in the lower extremity," *Journal of Biomechanics*, Vol. 30, pp. 1123-1131.
- Hardt, D.E, 1978. "Determining muscle forces in the leg during normal human walking – an application and evaluation of optimization methods," *Trans. Of ASME*. Vol. 100, pp.72-78.
- Hicks, J.L., Uchida, T.K., Seth, A., Rajagopal, A., Delp, S.L., 2015 "Is my model good enough? Best practices for verification and validation of musculoskeletal models and simulations of movement" *Journal of Biomechanical Engineering*, Vol. 137.

- John, C., Anderson, F., Higginson, C., Delp, S., 2012. "Stabilisation of walking by intrinsic muscle properties revealed in a three-dimensional muscle-driven simulation," *Computer Methods in Biomechanics & Biomedical Engineering*, Vol. 16, pp. 451-462.
- Kuster, M.S., 2002. "Exercise recommendations after total joint replacement," *Sports Medicine*. Vol. 32, pp. 433-445.
- Liu, M., Anderson, F., Schwartz, M., Delp, S., 2008. "Muscle contributions to support and progression over a range of walking speeds," *Journal of Biomechanics*, Vol. 41, pp. 3243-3252.
- MacConaill, M.A., 1967. "The ergonomic aspects of articular mechanics," *Studies of the Anatomy and Function of Bones and Joints*. pp. 69-80.
- Mantoan, A., Sartori, M., Sawacha, Z., Pizzolato, C., Cobelli, C., Reggiani, M., 2015. "MOtoNMS: A MATLAB toolbox to process motion data for neuromusculoskeletal modeling and simulation," *Source Code for Biology and Medicine*, Vol. 10, Issue 12.
- McHardy, A., Pollard, H., 2005. "Muscle activity during the golf swing," *British Journal of Sports Medicine*. Vol. 39, pp. 799-804.
- Morrison, J., 1970. "The mechanics of the knee joint in relation to normal walking," *Journal of Biomechanics*, Vol. 3, pp. 51-61.
- Moisio K.C., Sumner, D.R., Shott, S., Hurwitz, D.E., 2003. "Normalization of joint moments during gait: a comparison of two techniques," *Journal of Biomechanics*. Vol. 36. pp. 599-603.
- Mündermann, A., Dyrby, C.O., D'Lima, D.D., Colwell Jr., C.W., Andriacchi, T.P., 2008. "In vivo knee loading characteristics during activities of daily living as measured by an instrumented total knee replacement," *Journal of Orthopedic Research*. Vol. 26, pp. 1167-1172.
- Neptune, R., Kautz, S., Zajac, F., 2001. "Contributions of the individual ankle plantar flexors to support, forward progression, and swing initiation during walking," *Journal of Biomechanics*, Vol. 34, pp. 1387-1398.
- Newton, I., 1687. "Philosophiae Naturalis Principia Mathematica", The Royal Society Publications. London.
- OpenSim Documentation, 2019. <https://simtk-confluence.stanford.edu/display/OpenSim/OpenSim+Documentation>.
- Pandy, M., Andriacchi, T., 2010. "Muscle and joint function in human locomotion," *Annual Review of Biomedical Engineering*, Vol. 12, pp. 401-433.

- Patriarco, A.G., Mann, R.W., Simon, S.R., Mansour, J.M., 1981. "An evaluation of the approaches of optimization models in the prediction of muscle forces during human gait," *Journal of Biomechanics*, Vol. 14, pp. 513-525.
- Paul, J.P., 1965. "Bio-engineering studies of the forces transmitted by joints: II. Engineering analysis," *Biomechanics and Related Bio-engineering Topics*. pp. 369-380.
- Pfeiffer, J. L., Zhang, S., Milner, C., 2014. "Knee biomechanics during popular recreational and daily activities in older men," *The Knee*. Vol. 21, pp. 683-687.
- Seireg, A., Arvikar, R.J., 1975. "The prediction of muscular load sharing and joint forces in the lower extremities during walking," *Journal of Biomechanics*. Vol. 8, pp. 89-102.
- Shelburne, K., Pandy, M., Anderson, F., Torry, M., 2004. "Pattern of anterior cruciate ligament force in normal walking," *Journal of Biomechanics*, Vol. 37, pp. 797-805.
- Shelburne, K.B., Torry, M.R., Pandy, M.G., 2005. "Muscle, ligament, and joint-contact forces at the knee during walking," *Medicine & Science in Sports & Exercise*. Vol. 37, pp. 1948-1956.
- Shelburne, K.B., Torry, M.R., Pandy, M.G., 2006. "Contributions of muscles, ligaments, and the ground-reaction force to tibiofemoral joint loading during normal gait," *Journal of Orthopedic Research*. Vol. 24, pp. 1983-1990.
- Swanson, E.A., Schmalzried, T.P., Dorey, F.J., 2009. "Activity recommendations after total hip and knee arthroplasty: a survey of the American Association for Hip and Knee Surgeons," *The Journal of Arthroplasty*. Vol. 24, pp. 120-126.
- Vicon Motion Systems, 2019. <https://www.vicon.com/>
- Winter, D., 2009. *Biomechanics and motor control of human movement*. 4th ed., John Wiley & Sons, Inc., New Jersey.
- Winter, D., Sienko, S., 1988. "Biomechanics of below-knee amputee gait," *Journal of Biomechanics*, Vol. 21, pp. 361-367.
- Zajac, F.E., 1989. "Muscle and tendon: properties, models, scaling, and application to biomechanics and motor control," *Critical Reviews in Biomedical Engineering*, Vol. 17, pp. 359-411.
- Zajac, F.E., Neptune, R.R., Kautz, S.A., 2006. "Biomechanics and muscle coordination of human walking. Part 1: introduction to concepts, power transfer, dynamics and simulations," *Gait and Posture*. Vol. 16, pp. 215-232.

APPENDIX A

APPENDIX A

FUNDAMENTAL CHARACTERISTICS OF OPENSIM MODELS

OpenSim models can be characterized by the number of degrees-of-freedom and musculotendon actuators they possess. For the model used in this investigation, the generic 2392 musculoskeletal model was used (OpenSim Documentation, 2019). The pelvis was modeled as a rigid-body that has complete rotational and translational freedom which accounts for 6 dof. Each hip was modeled as a ball and socket joint, i.e. 3 dof each. The knee, modeled as a hinge joint, and the ankles containing 3 separate revolute joints, brings the total number of degrees-of-freedom to 20. The remaining 3 dof in the model represent the possible rotations of the HAT relative to the pelvis. Listed below is the complete list of the 92 musculotendon actuators represented in the model:

Muscle	Abbreviation	Gait 2392	Gait 2354
Gluteus Medius 1, Right	glut_med1_r	X	X
Gluteus Medius 2, Right	glut_med2_r	X	X
Gluteus Medius 2, Right	glut_med3_r	X	X
Gluteus Minimus 1, Right	glut_min1_r	X	
Gluteus Minimus 2, Right	glut_min2_r	X	
Gluteus Minimus 3, Right	glut_min3_r	X	
Semimembranosus, Right	semimem_r	X	
Semitendinosus, Right	semiten_r	X	
Biceps Femoris-Long Head, Right	bifemlh_r	X	X
Biceps Femoris-Short Head, Right	bifemsh_r	X	X
Sartorius, Right	sar_r	X	X
Adductor Longus, Right	add_long_r	X	
Adductor Brevis, Right	add_brev_r	X	
Adductor Magnus 1, Right	add_mag1_r	X	
Adductor Magnus 2, Right	add_mag2_r	X	X
Adductor Magnus 3, Right	add_mag3_r	X	
Tensor Fasciae Latae, Right	tfl_r	X	X
Pectineus, Right	pect_r	X	X
Gracilis, Right	grac_r	X	X
Gluteus Maximus 1, Right	glut_max1_r	X	X
Gluteus Maximus 2, Right	glut_max2_r	X	X
Gluteus Maximus 3, Right	glut_max3_r	X	X
Iliacus, Right	iliacus_r	X	X
Psoas Major, Right	psoas_r	X	X
Quadratus Femoris, Right	quad_fem_r	X	X
fixme gem, Right	gem_r	X	X
Piriformis, Right	peri_r	X	X
Rectus Femoris, Right	rect_fem_r	X	X
Vastus Medialis, Right	vas_med_r	X	
Vastus Intermedius, Right	vas_int_r	X	X
Vastus Lateralis, Right	vas_lat_r	X	
Medial Gastrocnemius, Right	med_gas_r	X	X
Lateral Gastrocnemius, Right	lat_gas_r	X	
Soleus, Right	soleus_r	X	X
Tibialis Posterior, Right	tib_post_r	X	X
Flexor Digitorum Longus, Right	flex_dig_r	X	
Flexor Hallucis Longus, Right	flex_hal_r	X	
Tibialis Anterior, Right	tib_ant_r	X	X
Peroneus Brevis, Right	per_brev_r	X	
Peroneus Longus, Right	per_long_r	X	
Peroneus Tertius, Right	per_tert_r	X	
Extensor Digitorum Longus, Right	ext_dig_r	X	
Extensor Hallucis Longus, Right	ext_hal_r	X	
Gluteus Medius 1, Left	glut_med1_l	X	
Gluteus Medius 2, Left	glut_med2_l	X	
Gluteus Medius 3, Left	glut_med3_l	X	
Gluteus Minimus 1, Left	glut_min1_l	X	
Gluteus Minimus 2, Left	glut_min2_l	X	
Gluteus Minimus 3, Left	glut_min3_l	X	
Semimembranosus, Left	semimem_l	X	
Semitendinosus, Left	semiten_l	X	
Biceps Femoris-Long Head, Left	bifemlh_l	X	

Biceps Femoris-Short Head, Left	bifemsh_l	X	
Sartorius, Left	sar_l	X	
Adductor Longus, Left	add_long_l	X	
Adductor Brevis, Left	add_brev_l	X	
Adductor Magnus 1, Left	add_mag1_l	X	
Adductor Magnus 2, Left	add_mag2_l	X	
Adductor Magnus 3, Left	add_mag3_l	X	
Tensor Fasciae Latae, Left	tfl_l	X	
Pectineus, Left	pect_l	X	
Gracilis, Left	grac_l	X	
Gluteus Maximus 1, Left	glut_max1_l	X	
Gluteus Maximus 2, Left	glut_max2_l	X	
Gluteus Maximus 3, Left	glut_max3_l	X	
Iliacus, Left	iliacus_l	X	
Psoas Major, Left	psoas_l	X	
Quadratus Femoris, Left	quad_fem_l	X	
fixme gem, Left	gem_l	X	
Piriformis, Left	peri_l	X	
Rectus Femoris, Left	rect_fem_l	X	
Vastus Medialis, Left	vas_med_l	X	
Vastus Intermedius, Left	vas_int_l	X	
Vastus Lateralis, Left	vas_lat_l	X	
Medial Gastrocnemius, Left	med_gas_l	X	
Lateral Gastrocnemius, Left	lat_gas_l	X	
Soleus, Left	soleus_l	X	
Tibialis Posterior, Left	tib_post_l	X	
Flexor Digitorum Longus, Left	flex_dig_l	X	
Flexor Hallucis Longus, Left	flex_hal_l	X	
Tibialis Anterior, Left	tib_ant_l	X	
Peroneus Brevis, Left	per_brev_l	X	
Peroneus Longus, Left	per_long_l	X	
Peroneus Tertius, Left	per_tert_l	X	
Extensor Digitorum Longus, Left	ext_dig_l	X	
Extensor Hallucis Longus, Left	ext_hal_l	X	
Erector Spinae, Right	ercspn_r	X	X
Erector Spinae, Left	ercspn_l	X	X
Internal Oblique, Right	intobl_r	X	X
Internal Oblique, Left	intobl_l	X	X
External Oblique, Right	extobl_r	X	X
External Oblique, Left	extobl_l	X	X

BIOGRAPHICAL SKETCH

Andrew B. Butler was born in Lafayette, IN on July 8, 1989. He graduated from Benjamin Franklin High School in New Orleans, LA in 2008. He then went on to earn a Bachelor of Science Degree in Biomedical Engineering from The University of Texas at Austin. Andrew received his Master of Science in Mechanical Engineering Degree at The University of Texas Rio Grande Valley in the Spring of 2019. He will be returning to industry and work as an Engineer following Graduation. His email address is a.b.butler@att.net.